

Dynamics of Decision Making in Animal Group Motion

Benjamin Nabet*, Naomi E. Leonard*, Iain D. Couzin[†] and Simon A. Levin[‡]

June 22, 2007

Abstract

We present a continuous model of a multi-agent system motivated by simulation studies on dynamics of decision making in animal groups in motion. Each individual moves at constant speed in the plane and adjusts its heading in response to relative headings of others in the population. Two subgroups of the population are informed such that individuals in each subgroup have a preferred direction of motion. The model exhibits fast and slow time scales allowing for a reduction in the dimension of the problem. The stable solutions for the reduced model correspond to compromise by individuals with conflicting preferences. We study the global phase space for the proposed reduced model by computing equilibria and proving stability and bifurcations.

1 INTRODUCTION

Recent research in cooperative control of groups of mobile autonomous agents has led to a growing effort to apply tools from dynamical systems and control theory toward better understanding how

*B. Nabet and N.E. Leonard are with the Department of Mechanical and Aerospace Engineering, Princeton University, Princeton, NJ, 08544 USA {bnabet,naomi}@princeton.edu. This work is supported in part by ONR grants N00014-02-1-0826 and N00014-04-1-0534.

[†]I.D. Couzin is with the Department of Zoology, South Parks Road, University of Oxford, Oxford, OX1 3PS, UK and the Department of Ecology and Evolutionary Biology, Princeton University, Princeton, NJ, 08544 USA icouzin@princeton.edu. This work was supported from the Royal Society, Balliol College and EPSRC grants GR/S04765/01 and GR/T11234/01.

[‡]S.A. Levin is with the Department of Ecology and Evolutionary Biology, Princeton University, Princeton, NJ, 08544 USA slevin@princeton.edu. This work was supported in part by DARPA grant HR0011-05-1-0057 and NSF grant EF-0434319.

biological systems manage collective tasks such as social foraging or migration. In this paper we derive and study the dynamics of a low-dimensional, minimally parameterized, coordinated control system, motivated by an interest in modelling and predicting the behavior of animal groups in motion. Many social organisms move in groups when they forage or migrate, and it is thought that the movement decisions they make may depend on social interactions among group members [1, 2, 3].

In Couzin et al [3], the mechanisms of decision-making and leadership are investigated using a discrete simulation of particles moving in the plane. In this simulation, each particle represents an individual animal and the motion of each individual is influenced by the state of its neighbors (e.g., relative position and relative heading). Within this group, there are two subgroups of informed individuals and one subgroup of naive individuals; each subgroup of informed individuals has a preferred direction of motion (representative of knowledge of location of food or migration route) that it can use to make decisions along with the information on its neighbors. It is shown in [3] that information can be transferred within groups even when there is no signaling, no identification of the informed individuals, and no evaluation of the information of individuals. It was also observed that with two informed subgroups of equal population, the direction of group motion depends on the degree to which the preferred directions differ. For low disagreement, the group follows the average preferred direction of all informed individuals, while for large disagreement the group selects one of the two preferred directions.

The model we propose and study in a simplified form in this paper corresponds to a deterministic set of ordinary differential equations. Each agent is modelled as a particle moving in the plane at constant speed with steering rate dependent on inter-particle measurements and, when appropriate, on prior information concerning preferred directions. The motivation from a biological point of view is to exploit the provable phase space dynamics of our simplified model to better understand and predict how movement decisions are made in animal groups.

This model is similar to models used for cooperative control of engineered multi-agent systems. For instance, a continuous model of particles moving at constant speed in the plane with steering control (heading rate) designed to couple the dynamics of the particles has been used for stabilization of circular and parallel collective motion [4, 5]. The use of the same kinds of models in the engineered and natural settings is no accident. The very efficient and robust ways that an-

imals move together and make collective decisions provide inspiration for design in engineering. Likewise, tools that have been developed for analysis and synthesis in the engineering context may prove useful for investigation in the natural setting. We note that the objectives in engineering applications may be analogous to objectives in the natural setting. For example, in the design of mobile sensor networks (such as the autonomous ocean sampling network described in [6]), the goal is to maximize information intake. This has parallels with optimal social foraging.

The central goal in the present work is to study the global phase space for the proposed simple model by computing equilibria and proving stability and bifurcations. Starting from a large-scale particle model, we reduce it to a simple planar model using a time-scale separation. Fast dynamics are associated with consensus of individuals with similar information and slow dynamics with the subsequent behavior of these different subgroups. In [7], the authors also use time-scale separation to reduce the dimension of consensus dynamics in complex networks. There the slow and fast time scales are due to sparse and dense connections among nodes in the network.

Our planar particle model includes key features of the discrete model of [3]; however, for the purpose of analysis, it is made simpler. For example, we first define our model for the full spatial dynamics and then we proceed to study only the dynamics of the headings. We prove the time scale separation for the model of the heading dynamics of two informed subgroups and one uninformed subgroup. For the bifurcation analysis of the slow dynamics, we focus our study on the two informed subgroups, and discuss the role of the uninformed individuals at the end of the paper. We study bifurcations as a function of two bifurcation parameter: $K \geq 0$, the coupling gain that weights the attention paid to neighbors versus the preferred direction, and $\bar{\theta}_2 \in [0, \pi]$, the relative angle of the two preferred directions.

In Section 2, we present the model. We identify fast and slow time scales and prove, for the system with two informed subgroup and one naive group, invariance and attractivity of the reduced (slow) manifold. In Section 3 we classify the equilibria of the reduced-order system with no naive individuals. In Section 4 we prove bifurcations in the system as a function of the coupling gain K . In Sections 5 and 6 we study two specific choices for the parameters K and $\bar{\theta}_2$ for which we can find a closed-form expression for the equilibrium points and compute analytically the bifurcation diagrams. In Section 7 we explain how the results change for unevenly sized groups of informed individuals and discuss future directions.

2 Models and time-scale separation

2.1 Particle model

We consider a population of N individuals each modeled as a particle moving in the plane. For the purpose of this paper, we assume that every individual can sense every other individual in the population. In the natural setting this all-to-all coupling assumption may be reasonably well justified for tightly clustered groups. A future objective will be to apply the theory in the case of limited sensing (see e.g., [8]).

The population is classified into three subgroups. Let N_1 and N_2 be the number of agents, respectively, in two different subgroups of informed individuals and let N_3 be the number of naive (uninformed) individuals such that $N_1 + N_2 + N_3 = N$. Let \mathcal{N}_1 and \mathcal{N}_2 , respectively, be the subset of indices in $\{1, \dots, N\}$ corresponding to individuals in subgroups 1 and 2 which comprise the two different groups of informed individuals. Let \mathcal{N}_3 be the remaining subset of indices corresponding to the naive individuals. Then the cardinality of \mathcal{N}_k is N_k , $k = 1, 2, 3$. The preferred heading direction for the individuals in subgroup i is denoted $\bar{\theta}_i$, for $i = 1, 2$.

We model each individual as a particle moving in the plane at constant speed. The heading direction of individual j is denoted θ_j , and θ_j is allowed to take any value in the circle S^1 . Let $r_j \in \mathbb{R}^2$ be the position of the j^{th} individual moving at constant speed V_0 , then

$$\dot{r}_j = (V_0 \cos \theta_j, V_0 \sin \theta_j), \quad j = 1, \dots, N.$$

Our simple model describes the dynamics of the heading angles for all individuals in the population independent of their positions. This model defines steering terms that depend only on relative heading angles. The dynamics are modelled as

$$\begin{aligned} \dot{\theta}_j &= \sin(\bar{\theta}_1 - \theta_j) + \frac{K}{N} \sum_{l=1}^N \sin(\theta_l - \theta_j), \quad j \in \mathcal{N}_1 \\ \dot{\theta}_j &= \sin(\bar{\theta}_2 - \theta_j) + \frac{K}{N} \sum_{l=1}^N \sin(\theta_l - \theta_j), \quad j \in \mathcal{N}_2 \\ \dot{\theta}_j &= \frac{K}{N} \sum_{l=1}^N \sin(\theta_l - \theta_j), \quad j \in \mathcal{N}_3. \end{aligned} \tag{1}$$

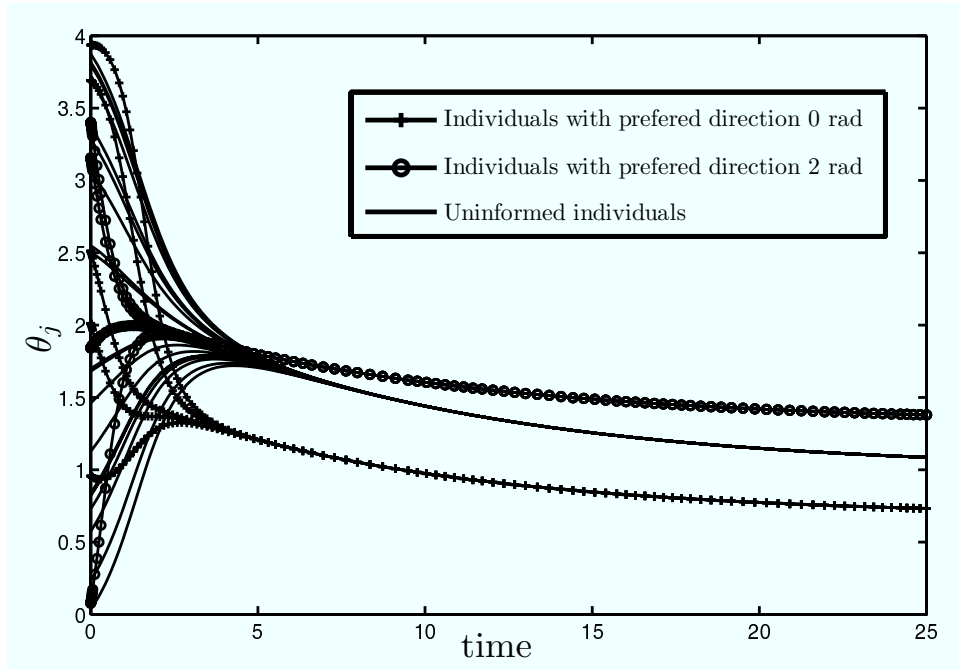


Figure 1: Phase angle of each individual in the group versus time for $K = 1$. For this simulation there are five individuals with preferred direction 0 rad, five individuals with preferred direction 2 rad and twenty individuals with no preferred direction. Two time scales in the dynamics can be observed. During a short initial transient time, the heading angles of the individuals in each subgroup synchronize. Then the three average subgroup directions change slowly to their steady state values.

We note that the form of the coupling is based on the Kuramoto model for populations of coupled oscillators [9]. The model is similar to that used by Mirollo and Strogatz to represent a group of coupled spins in a random magnetic field [10]. In the coupled spin model, there are no subgroups; instead, each individual oscillator has a randomly assigned “pinning” angle $\bar{\theta}_j$ such that the pinning angles are uniformly distributed around the circle. The studied system is known in physics as the mean-field theory for the random-field XY model, [11]. In [10] it is proven that the system exhibits a jump bifurcation and hysteresis as K is varied.

2.2 Model representation with two time scales

Now let $p_k \in \mathbb{C}$ denote the average of the phasors on the unit circle in the complex plane for the individuals in \mathcal{N}_k . In the coupled oscillator literature, p_k is known as the complex order parameter and $\rho_k := |p_k|$ provides a measure of synchrony among the phases. The average phasor p_k is

computed as

$$p_k = \rho_k e^{i\psi_k} = \frac{1}{N_k} \sum_{l \in \mathcal{N}_k} e^{i\theta_l}, \quad k = 1, 2, 3. \quad (2)$$

The parameter ρ_k takes values in the interval $[0, 1]$. It follows that $\rho_k = 1$ if all individuals in \mathcal{N}_k are heading in the same direction (synchronized headings) and $\rho_k = 0$ if individuals in \mathcal{N}_k head in directions such that their averaged velocity is zero. The average direction of individuals in \mathcal{N}_k is ψ_k .

Simulations of the model (1) shown in Figure 1, reveal two time scales in the dynamics. First, during a short initial transient time, the heading angles of the individuals in each subgroup synchronize. Then we observe a slow drift until the three average subgroup directions reach the steady state. Motivated by these observations, we define a new set of independent variables that distinguishes slow and fast variables. The average headings ψ_1, ψ_2 and ψ_3 are the slow variables since they characterize the lumped behavior of each of the three subgroups.

Following [12], the term $\frac{1}{N} \sum_{l=1}^N \sin(\theta_l - \theta_j)$, can be rewritten in terms of the complex order parameters as

$$\frac{1}{N} \sum_{l=1}^N \sin(\theta_l - \theta_j) = \frac{1}{N} \left(\sum_{k=1}^3 N_k \rho_k \sin(\psi_k - \theta_j) \right). \quad (3)$$

Using (3), the model (1) becomes

$$\begin{aligned} \dot{\theta}_j &= \sin(\bar{\theta}_1 - \theta_j) + \frac{K}{N} \left(\sum_{k=1}^3 N_k \rho_k \sin(\psi_k - \theta_j) \right), \quad j \in \mathcal{N}_1 \\ \dot{\theta}_j &= \sin(\bar{\theta}_2 - \theta_j) + \frac{K}{N} \left(\sum_{k=1}^3 N_k \rho_k \sin(\psi_k - \theta_j) \right), \quad j \in \mathcal{N}_2 \\ \dot{\theta}_j &= \frac{K}{N} \left(\sum_{k=1}^3 N_k \rho_k \sin(\psi_k - \theta_j) \right), \quad j \in \mathcal{N}_3. \end{aligned} \quad (4)$$

For $z_1, z_2 \in \mathbb{C}$, let $\langle z_1, z_2 \rangle = \Re\{z_1 z_2^*\}$. We further compute from (2) that

$$\langle p_k, ip_j \rangle = \langle \rho_k e^{i\psi_k}, i\rho_j e^{i\psi_j} \rangle = \frac{1}{N_k N_j} \left\langle \sum_{l \in \mathcal{N}_k} e^{i\theta_l}, \sum_{m \in \mathcal{N}_j} i e^{i\theta_m} \right\rangle,$$

which implies

$$\rho_k N_k \rho_j N_j \sin(\psi_j - \psi_k) = \sum_{l \in \mathcal{N}_k} \sum_{m \in \mathcal{N}_j} \sin(\theta_m - \theta_l). \quad (5)$$

The identity (5) is equal to zero if $j = k$. Similarly, for $k = 1, 2$,

$$\langle \rho_k e^{i\psi_k}, i e^{i\bar{\theta}_k} \rangle = \frac{1}{N_k} \sum_{l \in \mathcal{N}_k} \langle e^{i\theta_l}, i e^{i\bar{\theta}_k} \rangle,$$

which implies

$$\rho_k N_k \sin(\bar{\theta}_k - \psi_k) = \sum_{l \in \mathcal{N}_k} \sin(\bar{\theta}_k - \theta_l). \quad (6)$$

Using (1), (5) and (6) we can compute

$$\begin{aligned} \sum_{j \in \mathcal{N}_1} \dot{\theta}_j &= \rho_1 N_1 \sin(\bar{\theta}_1 - \psi_1) + \frac{K}{N} \rho_1 N_1 \rho_2 N_2 \sin(\psi_2 - \psi_1) + \frac{K}{N} \rho_1 N_1 \rho_3 N_3 \sin(\psi_3 - \psi_1) \\ \sum_{j \in \mathcal{N}_2} \dot{\theta}_j &= \rho_2 N_2 \sin(\bar{\theta}_2 - \psi_2) + \frac{K}{N} \rho_1 N_1 \rho_2 N_2 \sin(\psi_1 - \psi_2) + \frac{K}{N} \rho_2 N_2 \rho_3 N_3 \sin(\psi_3 - \psi_2) \\ \sum_{j \in \mathcal{N}_3} \dot{\theta}_j &= \frac{K}{N} \rho_1 N_1 \rho_3 N_3 \sin(\psi_1 - \psi_3) + \frac{K}{N} \rho_2 N_2 \rho_3 N_3 \sin(\psi_2 - \psi_3). \end{aligned}$$

To represent the fast dynamics, we define unit vectors as complex variables $\alpha_j \in \mathbb{C}$ where

$$\alpha_j = e^{i \left(N_k \theta_j - \sum_{l \in \mathcal{N}_k} \theta_l \right)}, \quad j \in \mathcal{N}_k.$$

Then,

$$\dot{\alpha}_j = i N_k \alpha_j \left(\dot{\theta}_j - \frac{1}{N_k} \sum_{l \in \mathcal{N}_k} \dot{\theta}_l \right), \quad j \in \mathcal{N}_k.$$

The unit vectors phasors α_j represent how much the heading of individual $j \in \mathcal{N}_k$ differs from ψ_k , the average direction of the subgroup k . When all the individuals in the k th subgroup have the same heading, $\alpha_j = 1, \forall j \in \mathcal{N}_k$. Denote $\boldsymbol{\theta} = (\theta_1, \dots, \theta_N) \in T^N$ and $\boldsymbol{\alpha}^k = (\alpha_{j(k,1)}, \dots, \alpha_{j(k, N_k-1)}) \in \mathbb{C}^{N_k-1}$, where $\mathcal{N}_k = \{j(k,1), \dots, j(k, N_k)\}$, and consider change of variables $\boldsymbol{\theta} \mapsto \{\boldsymbol{\alpha}^1, \boldsymbol{\alpha}^2, \boldsymbol{\alpha}^3, \psi_1, \psi_2, \psi_3\}$. Further, suppose $K \geq N \gg 1$ and let $\epsilon = 1/K$. We assume N_3 is of the same order or smaller than N , and N_1 and N_2 are both smaller than N , such that none of the following are as small as ϵ : $1/N_1, 1/N_2, N_1/N, N_2/N$. For example, in case $K = N = 100, N_1 = N_2 = 10, N_3 = 80$, then $\epsilon = 0.01$ and $1/N_1 = 1/N_2 = N_1/N = N_2/N = 0.1 = \sqrt{\epsilon}$. Given these assumptions, in the new

coordinates the coupled multi-agent system dynamics (1) become

$$\begin{aligned}\epsilon \dot{\alpha}_j &= iN_1 \alpha_j \left(\epsilon (\sin(\bar{\theta}_1 - \theta_j) - \rho_1 \sin(\bar{\theta}_1 - \psi_1)) + \frac{N_1}{N} \rho_1 \sin(\psi_1 - \theta_j) \right. \\ &\quad \left. + \sum_{k=2,3} \frac{N_k}{N} \rho_k (\sin(\psi_k - \theta_j) - \rho_1 \sin(\psi_k - \psi_1)) \right) \\ &=: g_j^1(\boldsymbol{\alpha}^1, \boldsymbol{\alpha}^2, \boldsymbol{\alpha}^3, \psi_1, \psi_2, \psi_3, \epsilon), \quad j \in \mathcal{N}_1, j \neq j_{(1, N_1)}\end{aligned}\quad (7)$$

$$\begin{aligned}\epsilon \dot{\alpha}_j &= iN_2 \alpha_j \left(\epsilon (\sin(\bar{\theta}_2 - \theta_j) - \rho_2 \sin(\bar{\theta}_2 - \psi_2)) + \frac{N_2}{N} \rho_2 \sin(\psi_2 - \theta_j) \right. \\ &\quad \left. + \sum_{k=1,3} \frac{N_k}{N} \rho_k (\sin(\psi_k - \theta_j) - \rho_2 \sin(\psi_k - \psi_2)) \right) \\ &=: g_j^2(\boldsymbol{\alpha}^1, \boldsymbol{\alpha}^2, \boldsymbol{\alpha}^3, \psi_1, \psi_2, \psi_3, \epsilon), \quad j \in \mathcal{N}_2, j \neq j_{(2, N_2)}\end{aligned}\quad (8)$$

$$\begin{aligned}\epsilon \dot{\alpha}_j &= iN_1 \alpha_j \left(\frac{N_3}{N} \rho_3 \sin(\psi_3 - \theta_j) + \sum_{k=2,3} \frac{N_k}{N} \rho_k (\sin(\psi_k - \theta_j) - \rho_3 \sin(\psi_k - \psi_3)) \right) \\ &=: g_j^3(\boldsymbol{\alpha}^1, \boldsymbol{\alpha}^2, \boldsymbol{\alpha}^3, \psi_1, \psi_2, \psi_3, \epsilon), \quad j \in \mathcal{N}_3, j \neq j_{(3, N_3)}\end{aligned}\quad (9)$$

$$\begin{aligned}\dot{\psi}_1 &= \frac{1}{\rho_1} \sum_{j \in \mathcal{N}_1} \left(\frac{1}{N_1} \sin(\bar{\theta}_1 - \theta_j) + \frac{K}{N} \left(\sum_{k=1}^3 \frac{N_k}{N_1} \rho_k \sin(\psi_k - \theta_j) \right) \right) \cos(\psi_1 - \theta_j) \\ &=: f_1(\boldsymbol{\alpha}^1, \boldsymbol{\alpha}^2, \boldsymbol{\alpha}^3, \psi_1, \psi_2, \psi_3, \epsilon)\end{aligned}\quad (10)$$

$$\begin{aligned}\dot{\psi}_2 &= \frac{1}{\rho_2} \sum_{j \in \mathcal{N}_2} \left(\frac{1}{N_2} \sin(\bar{\theta}_2 - \theta_j) + \frac{K}{N} \left(\sum_{k=1}^3 \frac{N_k}{N_2} \rho_k \sin(\psi_k - \theta_j) \right) \right) \cos(\psi_2 - \theta_j) \\ &=: f_2(\boldsymbol{\alpha}^1, \boldsymbol{\alpha}^2, \boldsymbol{\alpha}^3, \psi_1, \psi_2, \psi_3, \epsilon)\end{aligned}\quad (11)$$

$$\begin{aligned}\dot{\psi}_3 &= \frac{1}{\rho_3} \sum_{j \in \mathcal{N}_3} \left(\frac{K}{N} \left(\sum_{k=1}^3 \frac{N_k}{N_3} \rho_k \sin(\psi_k - \theta_j) \right) \right) \cos(\psi_3 - \theta_j) \\ &=: f_3(\boldsymbol{\alpha}^1, \boldsymbol{\alpha}^2, \boldsymbol{\alpha}^3, \psi_1, \psi_2, \psi_3, \epsilon)\end{aligned}\quad (12)$$

for $\rho_k \neq 0$, $k = 1, 2, 3$. In Appendix A we show that this change of coordinates is well defined.

The model (7)-(12) exhibits two time scales where the variables $\boldsymbol{\alpha}^1, \boldsymbol{\alpha}^2, \boldsymbol{\alpha}^3$ are the $N - 3$ fast variables and ψ_1, ψ_2, ψ_3 are the three slow variables. The solution $\alpha_j = 1$ for $j \in \mathcal{N}_k$, $k = 1, 2, 3$, equivalently $\theta_j = \psi_k$, $j \in \mathcal{N}_k$, $k = 1, 2, 3$, is an isolated solution of $g_j^k(\boldsymbol{\alpha}^1, \boldsymbol{\alpha}^2, \boldsymbol{\alpha}^3, \psi_1, \psi_2, \psi_3, 0) = 0$, $k = 1, 2, 3$. For this solution $\rho_k = 1$, $k = 1, 2, 3$. In other words, $\theta_j = \psi_k$, $j \in \mathcal{N}_k$, $k = 1, 2, 3$ is an invariant manifold of our system (1). Physically this means that if we start with all individuals

synchronized within their respective subgroup (i.e., $\theta_j = \psi_k$, $j \in \mathcal{N}_k$, $k = 1, 2, 3$), they will stay like this for all time. From the representation of the system dynamics (1) as equations (7)-(12) with $\epsilon \ll 1$, the corresponding slow dynamics, i.e., dynamics on the invariant manifold, are

$$\dot{\psi}_k = f_k(\boldsymbol{\alpha}^1 = \mathbf{1}, \boldsymbol{\alpha}^2 = \mathbf{1}, \boldsymbol{\alpha}^3 = \mathbf{1}, \psi_1, \psi_2, \psi_3, 0), \quad k = 1, 2, 3,$$

which can be written as

$$\begin{aligned} \dot{\psi}_1 &= \sin(\bar{\theta}_1 - \psi_1) + \frac{K}{N}N_2 \sin(\psi_2 - \psi_1) + \frac{K}{N}N_3 \sin(\psi_3 - \psi_1) \\ \dot{\psi}_2 &= \sin(\bar{\theta}_2 - \psi_2) + \frac{K}{N}N_1 \sin(\psi_1 - \psi_2) + \frac{K}{N}N_3 \sin(\psi_3 - \psi_2) \\ \dot{\psi}_3 &= \frac{K}{N}N_1 \sin(\psi_1 - \psi_3) + \frac{K}{N}N_2 \sin(\psi_2 - \psi_3). \end{aligned} \tag{13}$$

In Appendix B, we prove the reduction by proving the stability of the invariant manifold for the boundary layer dynamics. Singular perturbation theory (see e.g [13]) guarantees then that solutions to the unreduced dynamics stay close to solutions of the reduced system.

Consistent with the observations from simulations in [3], the solution of the fast dynamics corresponds to synchronization of all particle headings in subgroup k to common heading ψ_k , for $k = 1, 2, 3$. The slow dynamics, described by the reduced model (13), dictate the behavior of the common heading ψ_k of each of the three subgroups, $k = 1, 2, 3$. This reduced model is one in which all the agents in a subgroup (informed subgroups 1 and 2 and naive subgroup 3) behave as a single entity (thus the qualifier “lumped” model) and the inter-subgroup coupling term is weighted by the corresponding subgroup population size. This grouping of identical individuals, was also observed in the simulation from [3]. In that model, the grouping was spatial, each subgroup made a cluster within the group.

In the remaining sections of this paper, we focus our bifurcation analysis on the reduced dynamic model derived here. To further simplify this analysis, we first consider the case that $N_1 = N_2$ and $N_3 = 0$ (i.e. equal population for the two informed subgroups and no naive individuals) and then extend conclusions to the case $N_1 \neq N_2$, $N_3 = 0$ (i.e when one informed subgroup is more populated than the other and there are still no naive individuals). In the case $N_1 = N_2$ and $N_3 = 0$, (13)

becomes

$$\begin{aligned}\dot{\psi}_1 &= \sin(\bar{\theta}_1 - \psi_1) + \frac{K}{2} \sin(\psi_2 - \psi_1) \\ \dot{\psi}_2 &= \sin(\bar{\theta}_2 - \psi_2) + \frac{K}{2} \sin(\psi_1 - \psi_2).\end{aligned}\tag{14}$$

This model also corresponds to be the reduced dynamics in the case $N_1 = N_2 \gg 1$ and $K \geq 0$ not necessarily large. Without loss of generality we set $\bar{\theta}_1 = 0$. The two bifurcation parameters are $K \geq 0$ and $\bar{\theta}_2 \in [0, \pi]$. We note that the general reduced system (13) is a gradient system. In the case of $N_1 = N_2$ and $N_3 = 0$, the dynamics (14) are gradient dynamics such that

$$\dot{\psi}_k = -\frac{\partial V}{\partial \psi_k},$$

where V is given by

$$V(\psi_1, \psi_2) = -\cos \psi_1 - \cos(\bar{\theta}_2 - \psi_2) - \frac{K}{2} \cos(\psi_2 - \psi_1).$$

Thus, by LaSalle's Invariance Principle, all solutions converge to the set of critical points of $V(\psi_1, \psi_2)$ and there are no periodic solutions.

3 Equilibria

We first compute the equilibria of the system (14) but note that, in general, we cannot find closed form expressions for all of them. The equilibria are given by

$$\begin{aligned}-\sin \psi_1 + \frac{K}{2} \sin(\psi_2 - \psi_1) &= 0 \\ \sin(\bar{\theta}_2 - \psi_2) + \frac{K}{2} \sin(\psi_1 - \psi_2) &= 0.\end{aligned}$$

There are two sets of solutions, the first set given by

$$\begin{aligned}\psi_1 &= \pi - \bar{\theta}_2 + \psi_2 \\ \sin(\psi_2 - \bar{\theta}_2) &= \frac{K}{2} \sin \bar{\theta}_2,\end{aligned}\tag{15}$$

and the second set given by

$$\psi_1 = \bar{\theta}_2 - \psi_2 \quad (16)$$

$$\sin(\bar{\theta}_2 - \psi_2) = \frac{K}{2} \sin(2\psi_2 - \bar{\theta}_2). \quad (17)$$

First set of solutions Equation (15) has two solutions: $\psi_2 = \bar{\theta}_2 + \arcsin\left(\frac{K}{2} \sin \bar{\theta}_2\right)$ and $\psi_2 = \pi + \bar{\theta}_2 - \arcsin\left(\frac{K}{2} \sin \bar{\theta}_2\right)$. These two solutions exist if and only if $\left|\frac{K}{2} \sin \bar{\theta}_2\right| \leq 1$.

Lemma 3.1 *If $\left|\frac{K}{2} \sin \bar{\theta}_2\right| < 1$, the two equilibria $\boldsymbol{\psi}_{S1} = (\psi_1, \psi_2)_{S1}$ and $\boldsymbol{\psi}_{S2} = (\psi_1, \psi_2)_{S2}$ satisfying (15) given by*

$$\boldsymbol{\psi}_{S1} = \left(\pi + \arcsin\left(\frac{K}{2} \sin \bar{\theta}_2\right), \bar{\theta}_2 + \arcsin\left(\frac{K}{2} \sin \bar{\theta}_2\right) \right), \quad (18)$$

$$\boldsymbol{\psi}_{S2} = \left(-\arcsin\left(\frac{K}{2} \sin \bar{\theta}_2\right), \pi + \bar{\theta}_2 - \arcsin\left(\frac{K}{2} \sin \bar{\theta}_2\right) \right), \quad (19)$$

are saddle points $\forall K > 0$ and $\forall \bar{\theta}_2 \in [0, \pi]$. If $\frac{K}{2} \sin \bar{\theta}_2 = 1$, then $\boldsymbol{\psi}_{S1} = \boldsymbol{\psi}_{S2}$. In this case, if also $K > 0$ and $\bar{\theta}_2 \in (0, \frac{\pi}{2}) \cup (\frac{\pi}{2}, \pi)$ then $\boldsymbol{\psi}_{S1} = \boldsymbol{\psi}_{S2}$ is unstable with one zero eigenvalue and one positive real eigenvalue. If $\bar{\theta}_2 = \frac{\pi}{2}$ (and $K = 2$) then both eigenvalues are zero.

Proof: We compute the linearization of (14) at each of these two equilibria and show that its eigenvalues are always real and of opposite sign. The Jacobian of the system (14) is given by

$$J = \begin{pmatrix} -\cos \psi_1 - \frac{K}{2} \cos(\psi_2 - \psi_1) & \frac{K}{2} \cos(\psi_2 - \psi_1) \\ \frac{K}{2} \cos(\psi_2 - \psi_1) & -\cos(\bar{\theta}_2 - \psi_2) - \frac{K}{2} \cos(\psi_2 - \psi_1) \end{pmatrix}. \quad (20)$$

When we evaluate this matrix at either one of the two equilibria $\boldsymbol{\psi}_{S1}$ or $\boldsymbol{\psi}_{S2}$, we get

$$J|_{\boldsymbol{\psi}_{Si}} = \begin{pmatrix} \frac{K}{2} \cos \bar{\theta}_2 + \sqrt{1 - \frac{K^2}{4} \sin^2 \bar{\theta}_2} & -\frac{K}{2} \cos \bar{\theta}_2 \\ -\frac{K}{2} \cos \bar{\theta}_2 & \frac{K}{2} \cos \bar{\theta}_2 - \sqrt{1 - \frac{K^2}{4} \sin^2 \bar{\theta}_2} \end{pmatrix}.$$

Since the Jacobian is symmetric, the eigenvalues are real. The product of the two eigenvalues is

$$\lambda_1 \lambda_2 = \frac{K^2}{4} \sin^2 \bar{\theta}_2 - 1 < 0 \quad \text{for} \quad \left| \frac{K}{2} \sin \bar{\theta}_2 \right| < 1.$$

Therefore, for $\bar{\theta}_2 \in [0, \pi]$ the eigenvalues of the linearization are real and of opposite sign. This implies that equilibria ψ_{S1} and ψ_{S2} , if $\frac{K}{2} \sin \bar{\theta}_2 < 1$, are saddle points $\forall K > 0$ and $\forall \bar{\theta}_2 \in [0, \pi]$. In the case $|\frac{K}{2} \sin \bar{\theta}_2| = 1$, $\psi_{S1} = \psi_{S2} = (\frac{3\pi}{2}, \frac{\pi}{2} + \bar{\theta}_2)$ and we get for the Jacobian

$$J|_{\psi_{Si}} = \begin{pmatrix} \frac{K}{2} \cos \bar{\theta}_2 & -\frac{K}{2} \cos \bar{\theta}_2 \\ -\frac{K}{2} \cos \bar{\theta}_2 & \frac{K}{2} \cos \bar{\theta}_2 \end{pmatrix}.$$

The eigenvalues are $\lambda_1 = 0$ and $\lambda_2 = K \cos \bar{\theta}_2 > 0$. Therefore for $\bar{\theta}_2 \in (0, \frac{\pi}{2}) \cup (\frac{\pi}{2}, \pi)$, we have $\psi_{S1} = \psi_{S2} = (\frac{3\pi}{2}, \frac{\pi}{2} + \bar{\theta}_2)$ and the linearization is unstable with one zero eigenvalue and one strictly positive eigenvalue. In case $\bar{\theta}_2 = \pi/2$ and $K = 2$, $\lambda_1 = \lambda_2 = 0$. \square

The case in which $\bar{\theta}_2 = \frac{\pi}{2}$ is studied further in Section 4.2.

Second set of solutions In order to study (16)-(17) we make a change of variables $(\psi_1, \psi_2) \mapsto (\rho, \Psi)$ where $\rho \in [0, 1]$ and $\Psi \in S^1$ are defined by

$$\rho e^{i\Psi} = \frac{1}{2} (e^{i\psi_1} + e^{i\psi_2}). \quad (21)$$

Expanding this out and using (16) we compute

$$\begin{aligned} \rho (\cos \Psi + i \sin \Psi) &= \frac{1}{2} (\cos \psi_1 + \cos \psi_2) + \frac{1}{2} i (\sin \psi_1 + \sin \psi_2) \\ &= \cos \left(\frac{\psi_1 - \psi_2}{2} \right) \cos \left(\frac{\psi_1 + \psi_2}{2} \right) + i \cos \left(\frac{\psi_1 - \psi_2}{2} \right) \sin \left(\frac{\psi_1 + \psi_2}{2} \right) \\ &= \cos \left(\frac{\bar{\theta}_2}{2} - \psi_2 \right) \left(\cos \frac{\bar{\theta}_2}{2} + i \sin \frac{\bar{\theta}_2}{2} \right). \end{aligned} \quad (22)$$

For $\bar{\theta}_2 \in [0, \pi]$, (22) implies that $\Psi = \frac{\bar{\theta}_2}{2}$ or $\Psi = \frac{\bar{\theta}_2}{2} + \pi$. We can rewrite (17) as

$$\sin \frac{\bar{\theta}_2}{2} \cos \left(\frac{\bar{\theta}_2}{2} - \psi_2 \right) + \cos \frac{\bar{\theta}_2}{2} \sin \left(\frac{\bar{\theta}_2}{2} - \psi_2 \right) + K \sin \left(\frac{\bar{\theta}_2}{2} - \psi_2 \right) \cos \left(\frac{\bar{\theta}_2}{2} - \psi_2 \right) = 0. \quad (23)$$

In Section 6 we study the special case $\bar{\theta}_2 = \pi$. Here we focus on $\bar{\theta}_2 \in [0, \pi)$.

For $\Psi = \frac{\bar{\theta}_2}{2}$, (22) implies that $\cos \left(\frac{\bar{\theta}_2}{2} - \psi_2 \right) = \rho$ and $\sin \left(\frac{\bar{\theta}_2}{2} - \psi_2 \right) = \pm \sqrt{1 - \rho^2}$. Accordingly,

(23) implies that ρ satisfies

$$\rho \sin \frac{\bar{\theta}_2}{2} + \sqrt{1 - \rho^2} \cos \frac{\bar{\theta}_2}{2} + K\rho\sqrt{1 - \rho^2} = 0 \quad (24)$$

or

$$\rho \sin \frac{\bar{\theta}_2}{2} - \sqrt{1 - \rho^2} \cos \frac{\bar{\theta}_2}{2} - K\rho\sqrt{1 - \rho^2} = 0. \quad (25)$$

These imply that $\rho = 1$ if and only if $\bar{\theta}_2 = 0$, and $\rho = 0$ if and only if $\bar{\theta}_2 = \pi$. For $\bar{\theta}_2 \in (0, \pi)$, equation (24) does not have any solution for $\rho \in (0, 1)$ since every term on the left is positive, and equation (25) has one solution for $\rho \in (0, 1)$. We call the corresponding equilibrium $\boldsymbol{\psi}_{sync1} := (\psi_1, \psi_2)_{sync1}$. In the case $\bar{\theta}_2 = 0$, $\boldsymbol{\psi}_{sync1} = (0, 0)$.

Lemma 3.2 *The equilibrium $\boldsymbol{\psi}_{sync1}$ is a stable node for all $(K, \bar{\theta}_2) \in [0, \infty) \times [0, \pi)$.*

Proof: In order to prove this result, we show that the Jacobian has both eigenvalues real and negative. Using $\cos\left(\frac{\bar{\theta}_2}{2} - \psi_2\right) = \rho$ and $\sin\left(\frac{\bar{\theta}_2}{2} - \psi_2\right) = -\sqrt{1 - \rho^2}$ we can write the Jacobian evaluated at this equilibrium as

$$J|_{\boldsymbol{\psi}_{sync1}} = \begin{pmatrix} -\left(\rho \cos \frac{\bar{\theta}_2}{2} + \sqrt{1 - \rho^2} \sin \frac{\bar{\theta}_2}{2} + \frac{K}{2} (2\rho^2 - 1)\right) & \frac{K}{2} (2\rho^2 - 1) \\ \frac{K}{2} (2\rho^2 - 1) & -\left(\rho \cos \frac{\bar{\theta}_2}{2} + \sqrt{1 - \rho^2} \sin \frac{\bar{\theta}_2}{2} + \frac{K}{2} (2\rho^2 - 1)\right) \end{pmatrix}.$$

Since the diagonal matrix elements are equal and the off diagonal elements are equal, the eigenvalues are the sum and difference of these elements:

$$\lambda_{1,2} = -\left(\rho \cos \frac{\bar{\theta}_2}{2} + \sqrt{1 - \rho^2} \sin \frac{\bar{\theta}_2}{2} + \frac{K}{2} (2\rho^2 - 1)\right) \pm \frac{K}{2} (2\rho^2 - 1).$$

We find using (25) for all $(K, \bar{\theta}_2) \in [0, \infty) \times [0, \pi)$ that

$$-\sqrt{1 - \rho^2} \sin \frac{\bar{\theta}_2}{2} - K (2\rho^2 - 1) = -\frac{1}{\rho} (1 - \rho^2) \cos \frac{\bar{\theta}_2}{2} - K\rho^2 < 0. \quad (26)$$

Thus, for all $(K, \bar{\theta}_2) \in [0, \infty) \times [0, \pi)$, using (26) both eigenvalues are real and negative. Hence $\boldsymbol{\psi}_{sync1}$ is a stable node for all $(K, \bar{\theta}_2) \in [0, \infty) \times [0, \pi)$. \square

For $\Psi = \frac{\bar{\theta}_2}{2} + \pi$, (22) implies that $\cos\left(\frac{\bar{\theta}_2}{2} - \psi_2\right) = -\rho$ and $\sin\left(\frac{\bar{\theta}_2}{2} - \psi_2\right) = \pm\sqrt{1 - \rho^2}$. Hence,

by (23) ρ has to satisfy

$$-\rho \sin \frac{\bar{\theta}_2}{2} + \sqrt{1 - \rho^2} \cos \frac{\bar{\theta}_2}{2} - K\rho\sqrt{1 - \rho^2} = 0 \quad (27)$$

or

$$-\rho \sin \frac{\bar{\theta}_2}{2} - \sqrt{1 - \rho^2} \cos \frac{\bar{\theta}_2}{2} + K\rho\sqrt{1 - \rho^2} = 0. \quad (28)$$

Equation (27) has one solution for $\rho \in [0, 1]$; we call the corresponding equilibrium $\psi_{antisync1} := (\psi_1, \psi_2)_{antisync1}$.

Lemma 3.3 *The equilibrium $\psi_{antisync1}$ is unstable for all $(K, \bar{\theta}_2) \in [0, \infty) \times [0, \pi)$.*

Proof: In order to prove this result, we show that the Jacobian has at least one real, positive eigenvalue. Using $\cos\left(\frac{\bar{\theta}_2}{2} - \psi_2\right) = -\rho$ and $\sin\left(\frac{\bar{\theta}_2}{2} - \psi_2\right) = \sqrt{1 - \rho^2}$ we can write the Jacobian evaluated at this equilibrium as

$$J|_{\psi_{antisync1}} = \begin{pmatrix} \rho \cos \frac{\bar{\theta}_2}{2} + \sqrt{1 - \rho^2} \sin \frac{\bar{\theta}_2}{2} - \frac{K}{2} (2\rho^2 - 1) & \frac{K}{2} (2\rho^2 - 1) \\ \frac{K}{2} (2\rho^2 - 1) & \rho \cos \frac{\bar{\theta}_2}{2} + \sqrt{1 - \rho^2} \sin \frac{\bar{\theta}_2}{2} - \frac{K}{2} (2\rho^2 - 1) \end{pmatrix}.$$

The matrix has the same symmetry as in Lemma 3.2 and the eigenvalues can easily be computed to be

$$\lambda_{1,2} = \rho \cos \frac{\bar{\theta}_2}{2} + \sqrt{1 - \rho^2} \sin \frac{\bar{\theta}_2}{2} - \frac{K}{2} (2\rho^2 - 1) \pm \frac{K}{2} (2\rho^2 - 1).$$

One eigenvalue is equal to $\rho \cos \frac{\bar{\theta}_2}{2} + \sqrt{1 - \rho^2} \sin \frac{\bar{\theta}_2}{2} > 0$ for all $(K, \bar{\theta}_2) \in [0, \infty) \times [0, \pi)$. Hence $\psi_{antisync1}$ is unstable for all $(K, \bar{\theta}_2) \in [0, \infty) \times [0, \pi)$. \square

Equation (28) has between zero and two solutions for $\rho \in [0, 1]$, although we are not able to analytically find in general the range of parameters in which there are solutions nor the nature of their stability. The equilibria we get from (28) when they exist are called $\psi_{sync2} := (\psi_1, \psi_2)_{sync2}$ and $\psi_{antisync2} := (\psi_1, \psi_2)_{antisync2}$.

For all solutions (of the second set), in equations (25), (27) and (28), as K gets increasingly large, $K\rho\sqrt{1 - \rho^2}$ must approach zero. This means that as $K \rightarrow \infty$ then $\rho \rightarrow 0$ or $\rho \rightarrow 1$. We call an equilibrium *synchronized* if $\psi_1 = \psi_2 \bmod 2\pi$ and *anti-synchronized* if $\psi_1 - \psi_2 = \pi \bmod 2\pi$.

Thus, for very large values of K all the equilibria will be either *synchronized* ($\rho \rightarrow 1$) or *anti-synchronized* ($\rho \rightarrow 0$). For modest values of K , the strength of the coupling is less than or equal to the strength of the attraction to the preferred direction, and the equilibria are typically neither fully synchronized nor fully anti-synchronized. In this case we call an equilibrium *K -almost synchronized* (*K -almost anti-synchronized*) if the corresponding equilibrium in the case $K \gg 1$, is synchronized (anti-synchronized). Thus, K -almost synchronization occurs at $\Psi = \frac{\bar{\theta}_2}{2}$ and $\Psi = \frac{\bar{\theta}_2}{2} + \pi$. Note that these solutions correspond to an exact compromise between the two preferred directions.

Figure 2 shows two bifurcation diagrams in the cases (a) $\bar{\theta}_2 = 1$ rad and (b) $\bar{\theta}_2 = 2$ rad with bifurcation parameter K . The synchrony measure ρ as defined by (21), is plotted as a function of K for all equilibria in the second set of solutions. There are two equilibria that do not exist for low enough values of K ; these two equilibria are solution from (28). We also note in comparing Figures 2(a) and (b) that the stability of these two equilibria changes as a function of K and $\bar{\theta}_2$, indicating the presence of bifurcations. The other two equilibria can be seen to be defined for all values of K . The stable node is ψ_{sync1} which is the solution to (25). This equilibrium becomes synchronized as K increases, i.e., $\rho \rightarrow 1$ as $K \rightarrow \infty$. The unstable node is $\psi_{antisync1}$ which comes from (27). This equilibrium becomes anti-synchronized as K increases, i.e., $\rho \rightarrow 0$ as $K \rightarrow \infty$. As predicted above, it can be seen that as K increases ρ approaches 0 or 1 also for the two other equilibria.

4 Bifurcations in the (K, ψ_i) plane.

As we observed in Section 3, the system (14) undergoes bifurcations as we vary the two bifurcation parameters K and $\bar{\theta}_2$. For example, the two equilibria given by the first set of solutions, ψ_{S1} and ψ_{S2} , are defined if and only if $\frac{K}{2} \sin \bar{\theta}_2 \leq 1$. Also we recall that the equilibria given by equation (28) are not always defined and their stability type is dependent on the values of K and $\bar{\theta}_2$. In Section 5 we study the analytically solvable case $K = 2$. The case $\bar{\theta}_2 = \pi$, also solvable analytically, is treated in Section 6. In this section we consider bifurcations in K for $\bar{\theta}_2$ taking fixed value in three different intervals; first for $\frac{\pi}{2} < \bar{\theta}_2 < \pi$, then for $\bar{\theta}_2 = \frac{\pi}{2}$ and finally for $0 < \bar{\theta}_2 < \frac{\pi}{2}$. Figure 3 shows bifurcation diagrams with $\bar{\theta}_2$ fixed in each of these three intervals. The angle ψ_1 is plotted as a function of bifurcation parameter K . These plots are computed by solving numerically for the

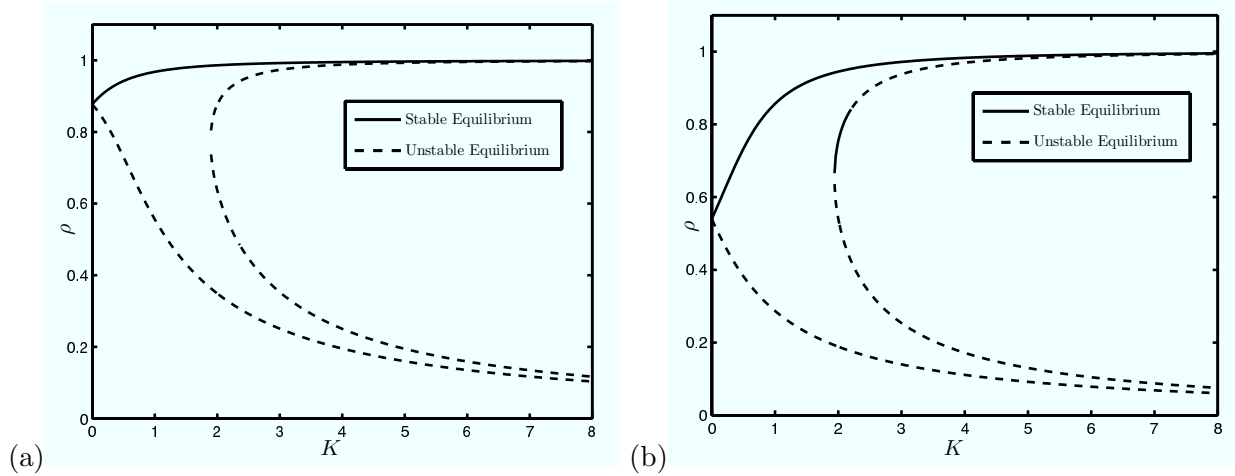


Figure 2: Bifurcation diagrams in cases (a) $\bar{\theta}_2 = 1$ rad and (b) $\bar{\theta}_2 = 2$ rad. The bifurcation parameter is K and ρ is plotted as a function of K for all equilibria in the second set of solutions. We note that two equilibria do not exist for low values of K . Stability of these same two equilibria changes type between (a) and (b), indicating the presence of bifurcations.

equilibria and characterizing the stability by computing the eigenvalues of the Jacobian.

4.1 Bifurcations in the (K, ψ_i) plane for $\frac{\pi}{2} < \bar{\theta}_2 < \pi$

The bifurcation diagram in the (K, ψ_i) plane for $\bar{\theta}_2 = \frac{3\pi}{4}$ is plotted in Figure 3(a). This is representative of the case $\frac{\pi}{2} < \bar{\theta}_2 < \pi$. There are two bifurcations: one at $K = K_1$ when two equilibria appear and one at $K = K_0 > K_1$ when two equilibria disappear. For $K_1 < K < K_0$ there are two stable equilibria whereas there is only one stable equilibrium when K is outside this region. The one stable equilibrium that exists for all $K \geq 0$ is ψ_{sync1} . The second stable equilibrium appears through a saddle node bifurcation, although we cannot find an analytic expression for K_1 , at which this bifurcation occurs. We can (partially) prove that the second stable equilibrium disappears through a hypercritical pitchfork at $K = K_0$. From Lemma 3.1, when $K = K_0 = 2/\sin \bar{\theta}_2$, the two equilibria ψ_{S1} and ψ_{S2} meet and are equal to $\psi_0 = (\psi_1, \psi_2)_0 = (\frac{3\pi}{2}, \bar{\theta}_2 + \frac{\pi}{2})$. For $K > K_0$, ψ_{S1} and ψ_{S2} no longer exist. With the change of variable $(\psi_1, \psi_2) \mapsto (\rho, \Psi)$ defined by (21) where $\rho \in [0, 1]$ and $\Psi \in S^1$, the equilibrium $\psi_{S1} = \psi_{S2} = \psi_0$ for $K = K_0$ becomes $(\rho, \Psi)_0 = (\sin \frac{\bar{\theta}_2}{2}, \frac{\bar{\theta}_2}{2} + \pi)$. This equilibrium also solves equation (28) and corresponds to ψ_{sync2} at $K = K_0$. Hence a third branch of equilibria from the second set of solutions goes through the bifurcation point $K = K_0$. It is easy to show that no other branch of equilibria crosses.

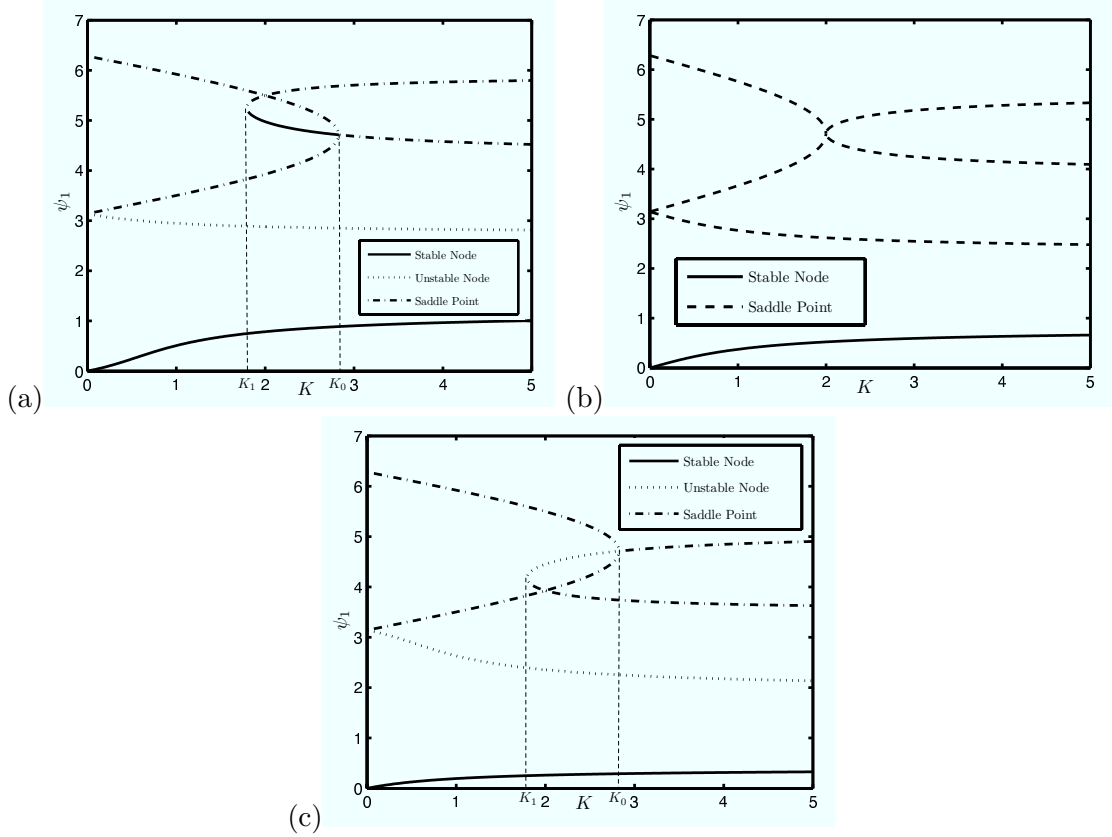


Figure 3: Bifurcation diagrams in cases (a) $\bar{\theta}_2 = \frac{3\pi}{4}$, (b) $\bar{\theta}_2 = \frac{\pi}{2}$ and (c) $\bar{\theta}_2 = \frac{\pi}{4}$. The bifurcation parameter is K and ψ_1 is plotted as a function of K for all equilibria of the system. We observe the hypercritical pitchfork bifurcation for $\bar{\theta}_2 = \frac{3\pi}{4}$ at $K = K_0$. For the case $\bar{\theta}_2 = \frac{\pi}{4}$, the bifurcation at $K = K_0$ only consists of a change in the number of equilibria but does not affect the stability of the system. In the case that $\bar{\theta}_2 = \frac{\pi}{2}$, the bifurcation only consists in the disappearance of two saddle points simultaneously with the appearance of two new ones.

In order to prove that the bifurcation $K = K_0$ is a *hypercritical pitchfork bifurcation*, we use the extension for pitchforks of the general theorem for saddle node bifurcations in [14]. However, of the three conditions to check in the theorem, we can verify only the first two. Thus, this is a partial proof.

1. *Non-degeneracy of the linearization.*

The linearization of (14) at $\psi = \psi_0$ and $K = K_0$ is

$$J_0 = \left. \frac{\partial \mathbf{f}}{\partial \psi} \right|_{\psi_0, K_0} = \cot \bar{\theta}_2 \begin{pmatrix} 1 & -1 \\ -1 & 1 \end{pmatrix}$$

where \mathbf{f} is the vector field given by (14) with corresponding state vector $\boldsymbol{\psi} = (\psi_1, \psi_2)$. This linearization is non-degenerate since it has a simple zero eigenvalue. We set $v = \begin{pmatrix} 1 \\ 1 \end{pmatrix}$ and $w = \begin{pmatrix} 1 & 1 \end{pmatrix}$ to be, respectively, the right and left eigenvectors of the linearization for the zero eigenvalue.

2. *Transversality condition to control non-degeneracy with respect to the parameter.*

For this condition we first check if the eigenvalues cross the imaginary axis with non-zero speed. We compute

$$\left. \frac{\partial^2 \mathbf{f}}{\partial \boldsymbol{\psi} \partial K} \right|_{\boldsymbol{\psi}_0, K_0} = \frac{1}{2} \cos \bar{\theta}_2 \begin{pmatrix} 1 & -1 \\ -1 & 1 \end{pmatrix}$$

which implies that $w \cdot \left. \frac{\partial^2 \mathbf{f}}{\partial \boldsymbol{\psi} \partial K} \right|_{\boldsymbol{\psi}_0, K_0} \cdot v = 0$. This means that the velocity (with respect to K) of the eigenvalues of the Jacobian (evaluated at $\boldsymbol{\psi}_{sync2} = \boldsymbol{\psi}_0$ and $K = K_0$) is zero when reaching the value zero (at the bifurcation). The conditions of this theorem are only sufficient though, we can still prove the bifurcation using the more general form of this condition. It remains to show that the equilibrium $\boldsymbol{\psi}_{sync2}$ goes from stable to unstable through the bifurcation. To do so we look at the eigenvalues of the Jacobian evaluated at $\boldsymbol{\psi}_{sync2}$ and show that the stability type of this equilibrium changes as K crosses the bifurcation value K_0 . Using equation (16), we can write the Jacobian evaluated at $\boldsymbol{\psi}_{sync2}$ as

$$\left. \frac{\partial \mathbf{f}}{\partial \boldsymbol{\psi}} \right|_{\boldsymbol{\psi}_{sync2}} = \begin{pmatrix} -\cos(\bar{\theta}_2 - \psi_2) - \frac{K}{2} \cos(2\psi_2 - \bar{\theta}_2) & \frac{K}{2} \cos(2\psi_2 - \bar{\theta}_2) \\ \frac{K}{2} \cos(2\psi_2 - \bar{\theta}_2) & -\cos(\bar{\theta}_2 - \psi_2) - \frac{K}{2} \cos(2\psi_2 - \bar{\theta}_2) \end{pmatrix} \Bigg|_{\boldsymbol{\psi}_{sync2}} \quad (29)$$

The eigenvalues are $\lambda_1 = -\cos(\bar{\theta}_2 - \psi_2)$ and $\lambda_2 = -\cos(\bar{\theta}_2 - \psi_2) - K \cos(2\psi_2 - \bar{\theta}_2)$. Since $\lambda_2|_{\boldsymbol{\psi}_0, K_0} = -\cos(\bar{\theta}_2 - \psi_2) - K \cos(2\psi_2 - \bar{\theta}_2)|_{\boldsymbol{\psi}_0, K_0} = \cot \bar{\theta}_2 < 0$ for $\bar{\theta}_2 > \frac{\pi}{2}$, we look for a change of sign of λ_1 through the bifurcation.

First we show that along the branch of equilibria corresponding to $\boldsymbol{\psi}_{sync2}$, near the bifurcation at $K = K_0$, ψ_2 is an increasing function of K , i.e., that $\left. \frac{\partial \psi_2}{\partial K} \right|_{\boldsymbol{\psi}_0, K_0} > 0$. Since on this branch of equilibria, equation (28) is satisfied, we take the partial derivative of both sides of (28)

with respect to K to get

$$\frac{\partial \rho}{\partial K} \left(-\sin \frac{\bar{\theta}_2}{2} + \frac{\rho}{\sqrt{1-\rho^2}} \cos \frac{\bar{\theta}_2}{2} + K\sqrt{1-\rho^2} - \frac{K\rho^2}{\sqrt{1-\rho^2}} \right) + \rho\sqrt{1-\rho^2} = 0. \quad (30)$$

Following the proof of Lemma 3.3, we can express on this branch ρ as a function of ψ_2 as

$$\rho = -\cos \left(\frac{\bar{\theta}_2}{2} - \psi_2 \right). \quad (31)$$

Taking partial derivative with respect to K of both sides of equation (31) gives

$$\frac{\partial \rho}{\partial K} = -\sin \left(\frac{\bar{\theta}_2}{2} - \psi_2 \right) \frac{\partial \psi_2}{\partial K}. \quad (32)$$

Substituting (32) into equation (30) gives

$$\frac{\partial \psi_2}{\partial K} = \frac{-\rho + \rho^3}{\sin \left(\frac{\bar{\theta}_2}{2} - \psi_2 \right) \left(\sqrt{1-\rho^2} \sin \frac{\bar{\theta}_2}{2} - \rho \cos \frac{\bar{\theta}_2}{2} - K + 2K\rho^2 \right)}.$$

At the bifurcation, we have

$$\left. \frac{\partial \psi_2}{\partial K} \right|_{\psi_0, K_0} = -\frac{1}{4} \sin \bar{\theta}_2 \tan \bar{\theta}_2 > 0 \quad \forall \bar{\theta}_2 > \frac{\pi}{2}, \quad (33)$$

i.e, about the bifurcation, on the branch of equilibria of ψ_{sync2} , for $\bar{\theta}_2 > \frac{\pi}{2}$, ψ_2 is a increasing function of K . Since $\lambda_1|_{\psi_{sync1}} = 0$ at $K = K_0$, then we can conclude that $\lambda_1|_{\psi_{sync2}} = -\cos(\bar{\theta}_2 - \psi_2)|_{\psi_{sync2}}$ is negative for $K < K_0$ and positive for $K > K_0$. Thus we have proved that ψ_{sync2} changes from stable node to saddle point through the bifurcation.

3. *Transversality condition to control non-degeneracy with respect to the dominant effect of the cubic nonlinear term.*

We first check this condition by computing

$$w_i v_j v_k v_l \left. \frac{\partial^3 f_i}{\partial \psi_j \partial \psi_k \partial \psi_l} \right|_{\psi_0, K_0} = 0,$$

for all $i, j, k, l \in \{1, 2\}$ and f_i is the i th component of the vector field \mathbf{f} given by (14). Since

these terms are all zero, this isn't sufficient to satisfy the condition. Instead, to prove the condition, we suggest to show that the dynamics on the center manifold have a non-degenerate cubic term. If this can successfully be carried out, we expect the sign of the cubic term to be positive proving that the bifurcation is a hypercritical pitchfork.

4.2 Bifurcations in the (K, ψ_i) plane for $\bar{\theta}_2 = \frac{\pi}{2}$

The bifurcation diagram in the (K, ψ_i) plane for $\bar{\theta}_2 = \frac{\pi}{2}$ is plotted in Figure 3(b). There is one bifurcation at $K = 2$ when two equilibria disappear and two new ones appear. This case is solvable analytically. The system (14) becomes

$$\begin{aligned}\dot{\psi}_1 &= -\sin \psi_1 + \frac{K}{2} \sin(\psi_2 - \psi_1) \\ \dot{\psi}_2 &= \sin\left(\frac{\pi}{2} - \psi_2\right) + \frac{K}{2} \sin(\psi_1 - \psi_2).\end{aligned}$$

From Section 3 we first observe that there is a bifurcation at $\frac{K}{2} \sin \bar{\theta}_2 = 1$, i.e, two equilibria in the first set disappear. For $\bar{\theta}_2 = \frac{\pi}{2}$, the bifurcation point is at $K = 2$.

4.2.1 Equilibria

Equation (17) at $\bar{\theta}_2 = \frac{\pi}{2}$ becomes $\cos \psi_2 = -\frac{K}{2} \cos(2\psi_2)$. After some trigonometric manipulation we can rewrite this equation as

$$K \cos^2 \psi_2 + \cos \psi_2 - \frac{K}{2} = 0. \tag{34}$$

We consider first the case that $K \in (0, 2)$. In this case equation (34) has two solutions

$$\psi_2 = \pm \arccos\left(\frac{-1 + \sqrt{1 + 2K^2}}{2K}\right).$$

This and the solutions of (15) give us a total of four equilibria as follows.

1. $\psi_{sync1} = \left(\frac{\pi}{2} - \arccos\left(\frac{-1 + \sqrt{1 + 2K^2}}{2K}\right), \arccos\left(\frac{-1 + \sqrt{1 + 2K^2}}{2K}\right)\right)$.

By Lemma 3.2, the equilibrium ψ_{sync1} is a *stable node* for $K \in (0, 2)$.

$$2. \psi_{\text{antisync1}} = \left(\frac{\pi}{2} - \arccos \left(\frac{-1 + \sqrt{1 + 2K^2}}{2K} \right), -\arccos \left(\frac{-1 + \sqrt{1 + 2K^2}}{2K} \right) \right).$$

By Lemma 3.3, the equilibrium $\psi_{\text{antisync1}}$ is an *unstable node* for $K \in (0, 2)$.

$$3. \psi_{S1} = \left(\frac{\pi}{2} + \arccos \left(-\frac{K}{2} \right), \arccos \left(-\frac{K}{2} \right) \right).$$

By Lemma 3.1, ψ_{S1} is a *saddle point* for all $K \in (0, 2)$.

$$4. \psi_{S2} = \left(\frac{\pi}{2} - \arccos \left(-\frac{K}{2} \right), -\arccos \left(-\frac{K}{2} \right) \right).$$

By Lemma 3.1, ψ_{S2} is a *saddle point* for all $K \in (0, 2)$.

We consider next the case that $K > 2$. The equilibria from the first set of solutions are not defined when $K > 2$ and $\bar{\theta}_2 = \frac{\pi}{2}$. Equation (34), in this case, has four solutions

$$\psi_2 = \pm \arccos \left(\frac{-1 \pm \sqrt{1 + 2K^2}}{2K} \right).$$

This gives us a total of four equilibria as follows.

$$1. \psi_{\text{sync1}} = \left(\frac{\pi}{2} - \arccos \left(\frac{-1 + \sqrt{1 + 2K^2}}{2K} \right), \arccos \left(\frac{-1 + \sqrt{1 + 2K^2}}{2K} \right) \right).$$

By Lemma 3.2, the equilibrium ψ_{sync1} is a *stable node* for $K > 2$.

$$2. \psi_{\text{antisync1}} = \left(\frac{\pi}{2} - \arccos \left(\frac{-1 + \sqrt{1 + 2K^2}}{2K} \right), -\arccos \left(\frac{-1 + \sqrt{1 + 2K^2}}{2K} \right) \right).$$

By Lemma 3.3, the equilibrium $\psi_{\text{antisync1}}$ is an *unstable node* for $K > 2$.

$$3. \psi_{\text{antisync2}} = \left(\frac{\pi}{2} - \arccos \left(\frac{-1 - \sqrt{1 + 2K^2}}{2K} \right), \arccos \left(\frac{-1 - \sqrt{1 + 2K^2}}{2K} \right) \right).$$

The Jacobian of the system evaluated at this equilibrium is

$$J = \frac{1}{2} \sqrt{1 - \left(\frac{-1 - \sqrt{1 + 2K^2}}{2K} \right)^2} \begin{pmatrix} -1 + \sqrt{1 + 2K^2} & -1 - \sqrt{1 + 2K^2} \\ -1 - \sqrt{1 + 2K^2} & -1 + \sqrt{1 + 2K^2} \end{pmatrix}.$$

The eigenvalues of this matrix are $\left\{ -\sqrt{1 - \left(\frac{-1 + \sqrt{1 + 2K^2}}{2K} \right)^2}, \sqrt{1 + 2K^2} \sqrt{1 - \left(\frac{-1 + \sqrt{1 + 2K^2}}{2K} \right)^2} \right\}$.

Hence the linearization has its eigenvalues of opposite sign $\forall K > 2$. The equilibrium $\psi_{\text{antisync2}}$

is a *saddle point* for all $K > 2$.

$$4. \psi_{\text{sync2}} = \left(\frac{\pi}{2} + \arccos \left(\frac{-1 - \sqrt{1 + 2K^2}}{2K} \right), -\arccos \left(\frac{-1 - \sqrt{1 + 2K^2}}{2K} \right) \right).$$

The Jacobian of the system evaluated at this equilibrium is

$$J = -\frac{1}{2} \sqrt{1 - \left(\frac{-1 - \sqrt{1 + 2K^2}}{2K} \right)^2} \begin{pmatrix} -1 + \sqrt{1 + 2K^2} & -1 - \sqrt{1 + 2K^2} \\ -1 - \sqrt{1 + 2K^2} & -1 + \sqrt{1 + 2K^2} \end{pmatrix}.$$

The eigenvalues of this matrix are $\left\{ \sqrt{1 - \left(\frac{-1 + \sqrt{1 + 2K^2}}{2K} \right)^2}, -\sqrt{1 + 2K^2} \sqrt{1 - \left(\frac{-1 + \sqrt{1 + 2K^2}}{2K} \right)^2} \right\}$.

Hence the linearization has its eigenvalues of opposite sign $\forall K > 2$. The equilibrium ψ_{sync2} is a *saddle point* for all $K > 2$.

4.2.2 Analysis of the bifurcation diagram

The analysis of the previous subsection shows that the bifurcation at $K = 2$ consists in the disappearance of two saddles (ψ_{S1} and ψ_{S2}), and the simultaneous appearance of two new saddles ($\psi_{antisync2}$ and ψ_{sync2}). At the bifurcation, these four equilibria come together at $(\psi_1, \psi_2)_{K=2, \bar{\theta}_2 = \frac{\pi}{2}} = (\frac{3\pi}{2}, \pi)$. This equilibrium is highly degenerate; the linearization J is equal to the zero matrix (see Lemma 3.1). This degenerate equilibrium will be encountered again in Section 5 when we set $K = 2$ and study bifurcation in the $(\bar{\theta}_2, \psi_i)$ plane. The $\bar{\theta}_2 = \frac{\pi}{2}$ plane studied here and the $K = 2$ plane studied in Section 5 are two orthogonal slices of the full parameter space $(K, \bar{\theta}_2, \psi_i)$.

4.3 Bifurcation in the (K, ψ_i) plane for $0 < \bar{\theta}_2 < \frac{\pi}{2}$

The bifurcation diagram in the (K, ψ_i) plane for $\bar{\theta}_2 = \frac{\pi}{4}$ is plotted in Figure 3(c). This is representative of the case $0 < \bar{\theta}_2 < \frac{\pi}{2}$. There are two bifurcations: one at $K = K_1$ when two equilibria appear and one at $K = K_0 > K_1$ when two equilibria disappear. For $K_1 < K < K_0$, there are two additional equilibria but the system still only has one stable equilibrium. We are not able to find an analytic expression of K_1 , at which the additional two equilibria appear from equation (28). However, we know we lose the two equilibria from the first set of solutions when $K_0 = 2/\sin \bar{\theta}_2$. Unlike the case of $\frac{\pi}{2} < \bar{\theta}_2 < \pi$ there is always one and only one stable equilibrium. When the two saddles from the first set of solution disappear, there is no pitchfork, rather the equilibrium from equation (28), $\psi_{antisync2}$, switches from being an unstable node to a saddle. To prove this we consider the linearization of the system near this bifurcation evaluated on the branch of the equilibria corresponding to $\psi_{antisync2}$. The eigenvalues of the Jacobian given by equation (29) are

$\lambda_1 = -\cos(\bar{\theta}_2 - \psi_2)$ and $\lambda_2 = -\cos(\bar{\theta}_2 - \psi_2) - K \cos(2\psi_2 - \bar{\theta}_2)$. For $\bar{\theta}_2 < \frac{\pi}{2}$, in some neighborhood of the bifurcation, $\lambda_2 > 0$ since $\lambda_2|_{\psi_0, K_0} = \cot \bar{\theta}_2 > 0$ for $\bar{\theta}_2 < \frac{\pi}{2}$. The eigenvalue λ_1 , as we saw in Section 4.1, changes sign through the bifurcation. In order to determine if the change is from positive to negative or negative to positive, we examine how ψ_2 changes as a function of K near the bifurcation. Using equation (33), we get

$$\left. \frac{\partial \psi_2}{\partial K} \right|_{\psi_0, K_0} = -\frac{1}{4} \sin \bar{\theta}_2 \tan \bar{\theta}_2 < 0, \quad \forall \bar{\theta}_2 \in \left(0, \frac{\pi}{2}\right).$$

Hence ψ_2 is a strictly decreasing function of K around the bifurcation. It is then easy to see that $\lambda_1|_{\psi_{antisync2}} = -\cos(\bar{\theta}_2 - \psi_2)|_{\psi_{antisync2}}$ becomes negative as K crosses the bifurcation value K_0 . This proves that $\psi_{antisync2}$ is an unstable node before the bifurcation and a saddle after the bifurcation. Thus, the disappearance of the saddles ψ_{S1} and ψ_{S2} at K_0 does not affect the stable equilibria of the system, only the number of unstable equilibria and the type of one unstable equilibrium.

5 Bifurcations in the case $K = 2$

In this section we set $K = 2$ and study the bifurcations in the $(\bar{\theta}_2, \psi_i)$ plane. This case is solvable analytically. In the model (14), $K = 2$ implies for each subgroup that the strength of the attraction towards the preferred direction is equal to the strength of the attraction to align with the other subgroup. The system (14) dynamics become

$$\begin{aligned} \dot{\psi}_1 &= -\sin \psi_1 + \sin(\psi_2 - \psi_1) \\ \dot{\psi}_2 &= \sin(\bar{\theta}_2 - \psi_2) - \sin(\psi_2 - \psi_1). \end{aligned}$$

5.1 Equilibria

For $K = 2$, equation (17) becomes $\sin(\bar{\theta}_2 - \psi_2) = \sin(2\psi_2 - \bar{\theta}_2)$. This equation has four solutions,

$$\psi_2 = \begin{cases} \frac{2}{3}\bar{\theta}_2 \\ \frac{2}{3}\bar{\theta}_2 + \frac{2\pi}{3} \\ \frac{2}{3}\bar{\theta}_2 + \frac{4\pi}{3} \\ \pi. \end{cases}$$

The system therefore has a total of six equilibria as follows.

1. $\psi_{sync1} = (\frac{1}{3}\bar{\theta}_2, \frac{2}{3}\bar{\theta}_2)$.

By Lemma 3.2, the equilibrium ψ_{sync1} is a *stable node* for $\bar{\theta}_2 \in [0, \pi]$.

2. $\psi_{sync2} = (\frac{1}{3}\bar{\theta}_2 - \frac{2\pi}{3}, \frac{2}{3}\bar{\theta}_2 + \frac{2\pi}{3})$.

The Jacobian of the system evaluated at this equilibrium is

$$J = \cos\left(\frac{1}{3}\bar{\theta}_2 - \frac{2\pi}{3}\right) \begin{pmatrix} -2 & 1 \\ 1 & -2 \end{pmatrix}.$$

The eigenvalues of this matrix are $\{-\cos(\frac{1}{3}\bar{\theta}_2 - \frac{2\pi}{3}), -3\cos(\frac{1}{3}\bar{\theta}_2 - \frac{2\pi}{3})\}$. Both eigenvalues are strictly positive for $\bar{\theta}_2 \in [0, \frac{\pi}{2})$, and both strictly negative for $\bar{\theta}_2 \in (\frac{\pi}{2}, \pi]$. The equilibrium ψ_{sync2} is an *unstable node* for $\bar{\theta}_2 \in [0, \frac{\pi}{2})$ and a *stable node* for $\bar{\theta}_2 \in (\frac{\pi}{2}, \pi]$.

3. $\psi_{antisync1} = (\frac{1}{3}\bar{\theta}_2 - \frac{4\pi}{3}, \frac{2}{3}\bar{\theta}_2 + \frac{4\pi}{3})$.

By Lemma 3.3, the equilibrium $\psi_{antisync1}$ is an *unstable node* for $\bar{\theta}_2 \in [0, \pi]$.

4. $\psi_{antisync2} = (\bar{\theta}_2 - \pi, \pi)$.

The Jacobian of the system evaluated at this equilibrium is

$$J = \cos \bar{\theta}_2 \begin{pmatrix} 0 & 1 \\ 1 & 0 \end{pmatrix}.$$

The eigenvalues of this matrix are $\{-\cos \bar{\theta}_2, \cos \bar{\theta}_2\}$ which are of opposite sign for all $\bar{\theta}_2 \in [0, \frac{\pi}{2}) \cup (\frac{\pi}{2}, \pi]$. So the equilibrium $\psi_{antisync2}$ is a *saddle point* for $\bar{\theta}_2 \in [0, \frac{\pi}{2}) \cup (\frac{\pi}{2}, \pi]$.

5. $\psi_{S1} = (\bar{\theta}_2 + \pi, 2\bar{\theta}_2)$.

By Lemma 3.1, the equilibrium ψ_{S1} is a *saddle point* for all $\bar{\theta}_2 \in [0, \frac{\pi}{2}) \cup (\frac{\pi}{2}, \pi]$.

6. $\psi_{S2} = (-\bar{\theta}_2, \pi)$.

By Lemma 3.1, the equilibrium ψ_{S2} is a *saddle point* for all $\bar{\theta}_2 \in [0, \frac{\pi}{2}) \cup (\frac{\pi}{2}, \pi]$.

Figure 4 shows an example of the six equilibria in the case $K = 2$ and $\bar{\theta}_2 = 1$ rad. The only stable equilibrium is ψ_{sync1} which for this example corresponds to motion in the $\Psi = .5$ rad direction.

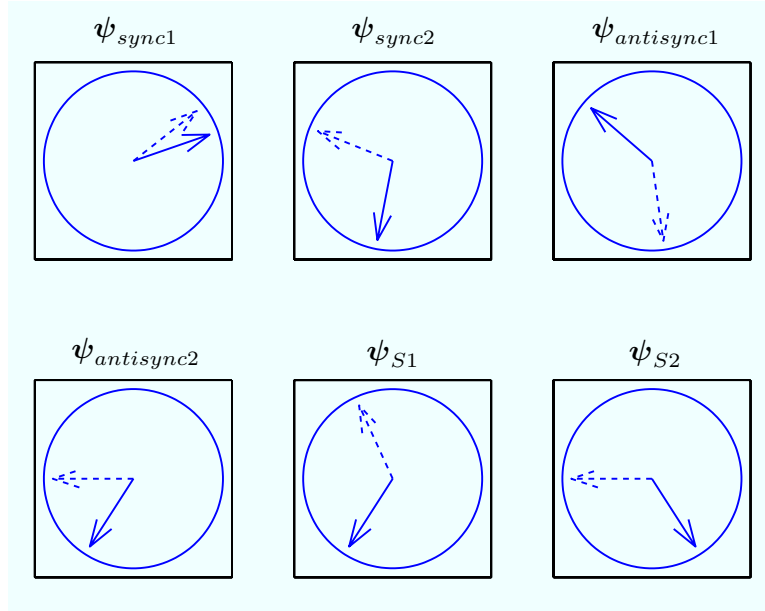


Figure 4: Picture of the six equilibria for $K = 2$ and $\bar{\theta}_2 = 1$ rad. The solid arrow represents ψ_1 on the unit circle, i.e., the average heading of the first informed subgroup, and the dashed arrow represents ψ_2 , the average heading of the second informed subgroup.

5.2 Analysis of the bifurcation diagram

The analysis of Section 5.1 shows that the stability type of one of the equilibria, ψ_{sync2} , changes at $\bar{\theta}_2 = \frac{\pi}{2}$ from an unstable node to a stable node. The equilibrium ψ_{sync2} for $\bar{\theta}_2 = \frac{\pi}{2}$ is a highly degenerate equilibrium; the linearization J is equal to the zero matrix. This is the same bifurcation point encountered in Section 4.2, but approached from an orthogonal direction in the full parameter space $(K, \bar{\theta}_2, \psi_i)$. Figure 5 shows the bifurcation diagram in the $(\bar{\theta}_2, \psi_1)$ plane, i.e, ψ_1 as a function of bifurcation parameter $\bar{\theta}_2$. In the bifurcation diagram (Figure 5) four equilibria come together at the point in phase space $(\psi_1, \psi_2) = (\frac{3\pi}{2}, \pi)$ when $\bar{\theta}_2 = \frac{\pi}{2}$. This bifurcation is one of Thom's seven

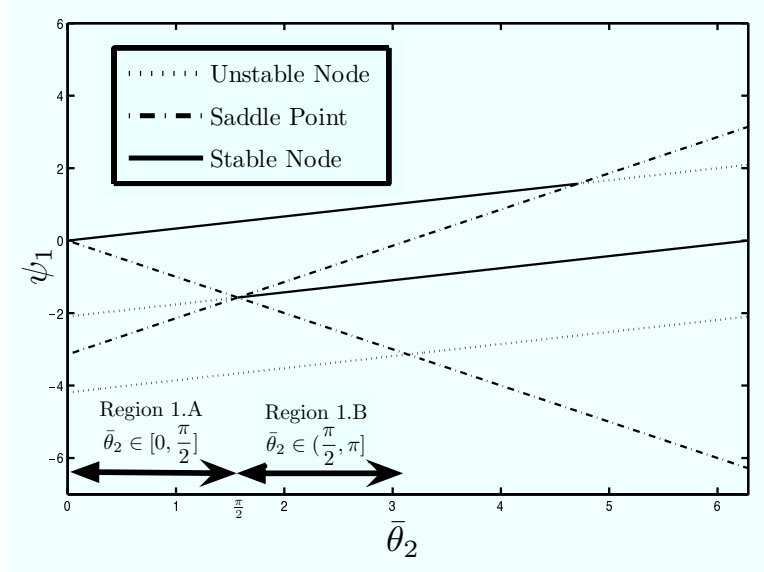


Figure 5: Bifurcation diagram in the $(\bar{\theta}_2, \psi_1)$ plane, i.e. ψ_1 as a function of bifurcation parameter $\bar{\theta}_2$ fixing $K = 2$. Since the equilibria $\psi_{antisync2}$ and ψ_{S1} have the same value for ψ_1 (but a different value for ψ_2), we see on this diagram only five equilibria even though there are six. At $\bar{\theta}_2 = \frac{\pi}{2}$ there are only three distinct equilibria; this is the degenerate point of the system. The multiplicity of the equilibrium $(\frac{3\pi}{2}, \pi)$ is four.

elementary catastrophes; it is called the *elliptic umbilic* [15].

Catastrophe theory applies to gradient systems, and the elementary catastrophes are classified by looking at the form of the potential. As discussed in Section 2, our system obeys gradient dynamics and the associated potential for $K = 2$ is

$$V = \cos \psi_1 + \cos (\bar{\theta}_2 - \psi_2) + \cos (\psi_1 - \psi_2). \quad (35)$$

To identify the bifurcation as an elliptic umbilic, we examine the unfolding of this potential near the catastrophe $(\psi_1, \psi_2, \bar{\theta}_2) = (\frac{3\pi}{2}, \pi, \frac{\pi}{2})$. We write (35) as

$$V = \cos \left(u + \frac{3\pi}{2} \right) + \cos \left(\frac{\pi}{2} + a - (\pi + v) \right) + \cos \left(u + \frac{3\pi}{2} - (\pi + v) \right), \quad (36)$$

where u, v and a are respectively the deviation of ψ_1 from $\frac{3\pi}{2}$, ψ_2 from π and $\bar{\theta}_2$ from $\frac{\pi}{2}$. A Taylor

expansion of (36), keeping terms up to third order in u and v gives

$$V = \frac{(\cos a - 1)}{3!}v^3 + \frac{uv^2}{2} - \frac{vu^2}{2} - \frac{\sin a}{2}v^2 + (1 - \cos a)v + \sin a.$$

After the following change of variables:

$$x = \frac{1}{2} \sqrt[3]{\frac{(4 \cos a - 1)}{3}} v$$

$$y = \sqrt[3]{\frac{2\sqrt{6}}{\sqrt{4 \cos a - 1}}} \left(\frac{1}{\sqrt{6}} u - \frac{1}{2\sqrt{6}} v \right),$$

the potential becomes

$$V = x^3 - 3xy^2 - \frac{2 \times 3^{\frac{2}{3}} \sin a}{(4 \cos a - 1)^{\frac{2}{3}}} x^2 - \frac{2 \times 3^{\frac{1}{3}} (\cos a - 1)}{(4 \cos a - 1)^{\frac{1}{3}}} x + \sin a. \quad (37)$$

In (37) we recognize the standard unfolding of the potential of an elliptic umbilic [16].

In the following paragraph we examine the different equilibria in each of the various regions of the bifurcation diagram shown in Figure 5. Region 1.A is defined by $\bar{\theta}_2 \in [0, \frac{\pi}{2}]$ and Region 1.B by $\bar{\theta}_2 \in (\frac{\pi}{2}, \pi]$. For each case studied, we draw the pictures of each possible equilibrium (stable and unstable) on the unit circle, a solid arrow corresponding to ψ_1 and a dashed arrow corresponding to ψ_2 . Because $K = 2$ implies equal attraction to the preferred direction as to the other subgroup, equilibria are usually not fully synchronized nor anti-synchronized. Instead the equilibria ψ_{sync1} and ψ_{sync2} are *K-almost synchronized* and $\psi_{antisync1}$ and $\psi_{antisync2}$ are *K-almost anti-synchronized*. Since ψ_{S1} and ψ_{S2} from (15) are not defined for $K \gg 1$, we cannot use this terminology. However, we note that the relative heading of ψ_1 and ψ_2 is equal to $\pi - \bar{\theta}_2$ for ψ_{S1} and $\pi + \bar{\theta}_2$ for ψ_{S2} independent of K . As $\bar{\theta}_2$ increases to π , the two saddles become synchronized. We call an equilibrium $\bar{\theta}_2$ -almost synchronized if the corresponding equilibrium in the case $\bar{\theta}_2 \rightarrow \pi$ is synchronized.

Region 1.A $\bar{\theta}_2 \in [0, \frac{\pi}{2}]$. The equilibria in the case $\bar{\theta}_2 \in [0, \frac{\pi}{2})$ are shown in Figure 6. Figure 7 shows the equilibria at the bifurcation point $\bar{\theta}_2 = \frac{\pi}{2}$. In Figure 6 there are three types of equilibria: the *K-almost synchronized* ψ_{sync1} and ψ_{sync2} , the *K-almost anti-synchronized* $\psi_{antisync1}$ and $\psi_{antisync2}$ and the $\bar{\theta}_2$ -almost synchronized ψ_{S1} and ψ_{S2} . The only stable equilibrium, ψ_{sync1} ,

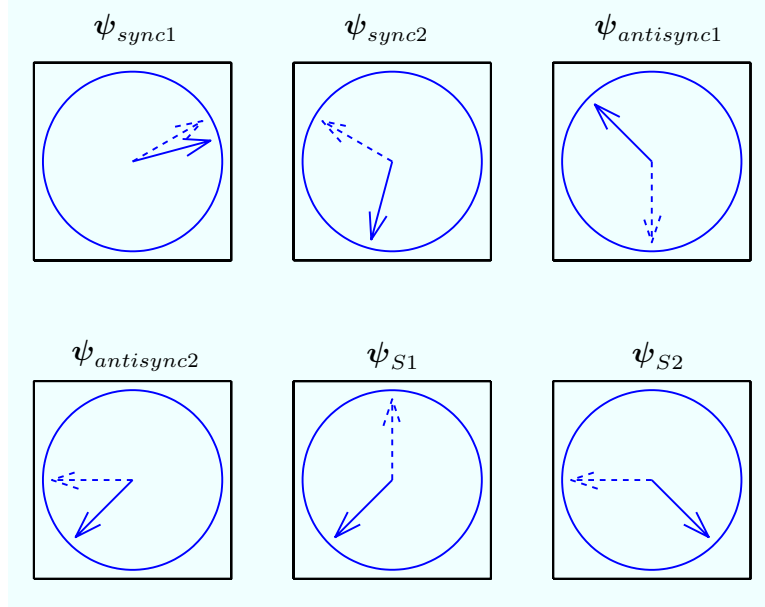


Figure 6: These diagrams show pictures of all the equilibria for $\bar{\theta}_2 = \frac{\pi}{4}$. This is representative of the possible equilibria for the system in Region 1A without its boundary, i.e., for $\bar{\theta}_2 \in [0, \frac{\pi}{2})$. The only stable equilibrium is ψ_{sync1} which for this example corresponds to motion in the $\Psi = \frac{\pi}{8}$ direction.

is the K -almost synchronized motion of ψ_1 and ψ_2 in the direction $\Psi = \frac{\bar{\theta}_2}{2}$ with each heading remaining on its side (nearest its preferred direction) of $\Psi = \frac{\bar{\theta}_2}{2}$. The unstable equilibria are the two K -almost anti-synchronized $\psi_{antisync1}$ and $\psi_{antisync2}$, the remaining K -almost synchronized ψ_{sync2} which flanks $\Psi = \frac{\bar{\theta}_2}{2} + \pi$ and the two $\bar{\theta}_2$ -almost synchronized saddles. The first saddle ψ_{S1} will tend to go closer to the preferred direction $\bar{\theta}_1 = 0$, and the second saddle ψ_{S2} will go closer to $\bar{\theta}_2$ as $\bar{\theta}_2 \rightarrow \pi$.

As mentioned previously, the case at the boundary $\bar{\theta}_2 = \frac{\pi}{2}$ is highly degenerate. There are only three distinct equilibria. There is still only one stable equilibrium which is K -almost synchronized at $\Psi = \frac{\bar{\theta}_2}{2} = \frac{\pi}{4}$. There is also an unstable K -almost anti-synchronized equilibrium $\psi_{antisync1}$ at $\Psi = \frac{\bar{\theta}_2}{2} + \pi = \frac{5\pi}{4}$. The other equilibrium corresponds to $\Psi = \frac{\bar{\theta}_2}{2} + \pi = \frac{5\pi}{4}$. As can be seen in the bifurcation diagram of Figure 5, there is the superposition of four equilibria ψ_{sync2} , ψ_{S1} , ψ_{S2} and $\psi_{antisync2}$. This equilibrium is called a *monkey-saddle* in the catastrophe theory literature [16].

Region 1.B $\bar{\theta}_2 \in (\frac{\pi}{2}, \pi]$. The equilibria in the case $\bar{\theta}_2 \in (\frac{\pi}{2}, \pi)$ are shown in Figure 8. Figure 9 shows the equilibria at the boundary $\bar{\theta}_2 = \pi$. In Figure 8 the equilibria are similar to those from the case where $\bar{\theta}_2 \in [0, \frac{\pi}{2})$ in Figure 6 except that now the K -almost synchronized equilibrium

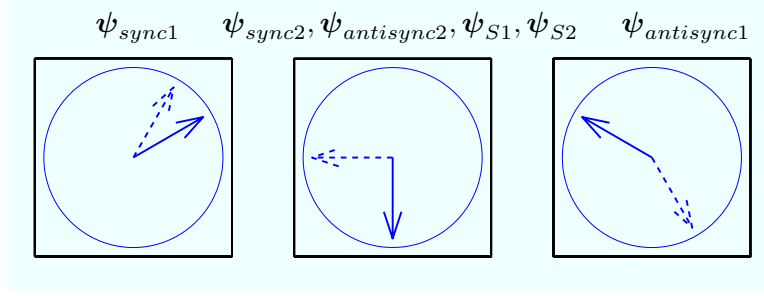


Figure 7: These diagrams show the equilibria of the system at the critical point, i.e when both $K = 2$ and $\bar{\theta}_2 = \frac{\pi}{2}$. We only have three equilibria. The second equilibrium drawn is the superposition of four equilibria ψ_{sync2} , $\psi_{antisync2}$, ψ_{S1} and ψ_{S2} ; it has multiplicity four. It is called a monkey-saddle in the catastrophe theory literature.

ψ_{sync2} at $\frac{\bar{\theta}_2}{2} + \pi$ is stable. Two of the unstable equilibria ($\psi_{antisync1}, \psi_{antisync2}$) are K -almost anti-synchronized. As mentioned above, for ψ_{S1} and ψ_{S2} , the particles synchronize as $\bar{\theta}_2$ increases; the saddle ψ_{S1} is closer to the preferred direction of the first particle and the saddle ψ_{S2} is closer to the preferred direction of the second particle.

In the case $\bar{\theta}_2 = \pi$ (Figure 9), there are still two stable equilibria ($\psi_{sync1}, \psi_{sync2}$) which are K -almost synchronized at $\Psi = \frac{\bar{\theta}_2}{2} = \frac{\pi}{2}$ and $\Psi = \frac{\bar{\theta}_2}{2} + \pi = \frac{3\pi}{2}$. The unstable equilibria $\psi_{antisync1}$ and $\psi_{antisync2}$ are anti-synchronized. The two saddles are synchronized: ψ_{S1} is synchronized at the preferred direction of the first particle ($\bar{\theta}_1 = 0$) and ψ_{S2} is synchronized at the preferred direction of the second particle ($\bar{\theta}_2 = \pi$).

6 Bifurcation in the (K, ψ_i) plane for $\bar{\theta}_2 = \pi$

In this section, we set $\bar{\theta}_2 = \pi$, and study the bifurcation in the (K, ψ_i) plane. This case is solvable analytically. For this case, the two preferred headings differ by 180 degrees. Since the disagreement is so large, for some range of small values of K the group will split without making any compromise. This kind of splitting is sometimes observed in swarm-bees [17]. The system (14) becomes

$$\begin{aligned}\dot{\psi}_1 &= -\sin \psi_1 + \frac{K}{2} \sin(\psi_2 - \psi_1) \\ \dot{\psi}_2 &= \sin \psi_2 + \frac{K}{2} \sin(\psi_1 - \psi_2).\end{aligned}\tag{38}$$

We note that this system appears in Chapter 8 of [18].

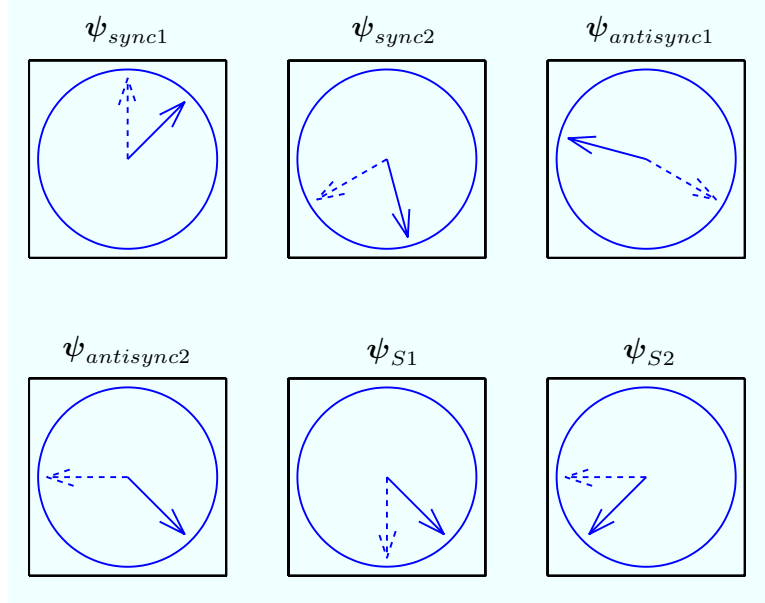


Figure 8: These diagrams show the pictures of all the equilibria for $\bar{\theta}_2 = \frac{3\pi}{4}$. This is representative of the possible equilibria for the system in Region 1B without its boundary i.e for $\bar{\theta}_2 \in (\frac{\pi}{2}, \pi)$. The two saddles, ψ_{S1} and ψ_{S2} , tend to be more synchronized (than in Figure 6) since $\bar{\theta}_2$ is closer to π . ψ_{S1} is closer to the preferred direction of the first subgroup and ψ_{S2} is closer to the preferred direction of the second subgroup. There are two stable equilibria, ψ_{sync1} and ψ_{sync2} .

6.1 Equilibria

For $\bar{\theta}_2 = \pi$, the equation (17) becomes $\sin \psi_2 = -\frac{K}{2} \sin(2\psi_2)$. After some trigonometric manipulation we can rewrite this equation as

$$\sin \psi_2 (1 + K \cos \psi_2) = 0. \quad (39)$$

We consider first the case that $K \in [0, 1)$. In this case equation (39) has two solutions

$$\psi_2 = \begin{cases} 0 \\ \pi. \end{cases}$$

This give us a total of four equilibria as follows.

1. $\psi_{antisync1} = (\pi, 0)$.

By Lemma 3.3, the equilibrium $\psi_{antisync1}$ is an *unstable node* for $K \in [0, 1]$.

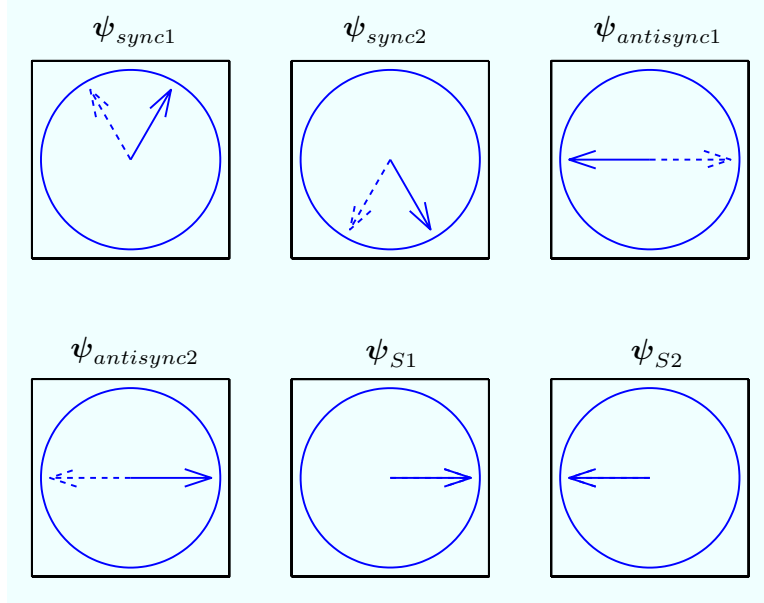


Figure 9: These diagrams show the equilibria of the system at the right boundary of Region 1.B, i.e., for $\bar{\theta}_2 = \pi$. Only equilibrium ψ_{sync1} and ψ_{sync2} (the K -almost synchronized equilibria) depend on K . The other equilibria are anti-synchronized ($\psi_{antisync1}$ and $\psi_{antisync2}$) or synchronized (ψ_{S1} and ψ_{S2}) for all K .

2. $\psi_{antisync2} = (0, \pi)$.

The Jacobian of the system evaluated at this equilibrium is

$$J = \begin{pmatrix} -1 + \frac{K}{2} & -\frac{K}{2} \\ -\frac{K}{2} & -1 + \frac{K}{2} \end{pmatrix}.$$

The eigenvalues of this matrix are $\{-1, -1 + K\}$. Hence the linearization has both eigenvalues strictly negative $\forall K \in [0, 1)$. The equilibrium $\psi_{antisync2}$ is a *stable node* $\forall K \in [0, 1)$.

3. $\psi_{S1} = (0, 0)$.

By Lemma 3.1, the equilibrium ψ_{S1} is a *saddle point* for all $K \in [0, 1]$.

4. $\psi_{S2} = (\pi, \pi)$.

By Lemma 3.1, the equilibrium ψ_{S2} is a *saddle point* for all $K \in [0, 1]$.

We consider next the case that $K > 1$. Equation (39), in this case has four solutions

$$\psi_2 = \begin{cases} \arccos\left(-\frac{1}{K}\right) \\ -\arccos\left(-\frac{1}{K}\right) \\ 0 \\ \pi. \end{cases}$$

This gives a total of six equilibria as follows

1. $\psi_{sync1} = (\pi - \arccos(-\frac{1}{K}), \arccos(-\frac{1}{K}))$.

By Lemma 3.2, the equilibrium ψ_{sync1} is a *stable node* for $K > 1$.

2. $\psi_{sync2} = (\pi + \arccos(-\frac{1}{K}), -\arccos(-\frac{1}{K}))$.

The Jacobian of the system evaluated at this equilibrium is

$$J = \begin{pmatrix} -\frac{K}{2} & -\frac{1}{K} + \frac{K}{2} \\ -\frac{1}{K} + \frac{K}{2} & -\frac{K}{2} \end{pmatrix}.$$

The eigenvalues of this matrix are $\{-\frac{1}{K}, \frac{1-K^2}{K}\}$. Hence the linearization has both eigenvalues strictly negative $\forall K > 1$. The equilibrium ψ_{sync2} is a *stable node* $\forall K > 1$.

3. $\psi_{antisync1} = (\pi, 0)$.

By Lemma 3.3, the equilibrium $\psi_{antisync1}$ is an *unstable node* for $K \geq 1$.

4. $\psi_{antisync2} = (0, \pi)$.

The Jacobian of the system evaluated at this equilibrium is

$$J = \begin{pmatrix} -1 + \frac{K}{2} & -\frac{K}{2} \\ -\frac{K}{2} & -1 + \frac{K}{2} \end{pmatrix}.$$

The eigenvalues of this matrix are $\{-1, -1 + K\}$. Hence the linearization has its eigenvalues of opposite sign $\forall K > 1$. The equilibrium $\psi_{antisync2}$ is a *saddle point* $\forall K > 1$.

5. $\psi_{S1} = (0, 0)$.

By Lemma 3.1, the equilibrium ψ_{S1} is a *saddle point* for all $K \geq 1$.

6. $\psi_{S2} = (\pi, \pi)$.

By Lemma 3.1, the equilibrium ψ_{S2} is a *saddle point* for all $K \geq 1$.

6.2 Analysis of the bifurcation diagram

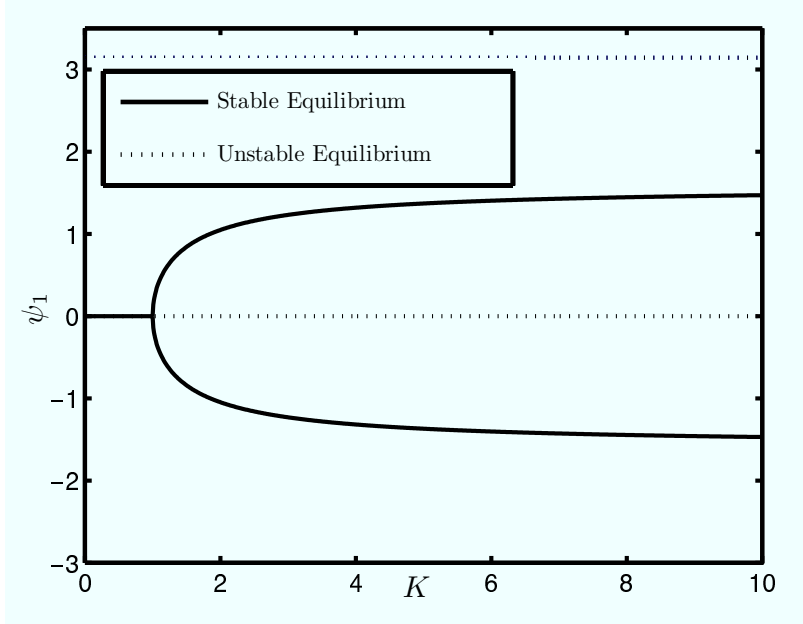


Figure 10: Bifurcation diagram in the (K, ψ_1) plane, i.e, ψ_1 as a function of bifurcation parameter K fixing $\bar{\theta}_2 = \pi$. At $K = 1$ we have a supercritical pitchfork bifurcation. We have one stable equilibrium for $K < 1$ and two stable equilibria for $K > 1$.

The analysis of the previous subsection, shows that a bifurcation occurs at $K = 1$. The bifurcation diagram (Figure 10), suggests that there is a *supercritical pitchfork bifurcation*. To prove this, we use the extension for pitchforks of the general theorem for saddle node bifurcations in [14]. There are three conditions to check in the theorem. We define $\psi_0 = (\psi_1, \psi_2)_0 = (0, \pi)$, $K_0 = 1$.

1. *Non-degeneracy of the linearization.*

The linearization of (38) at $\psi = \psi_0$ and $K = K_0$ is

$$J_0 = \left. \frac{\partial \mathbf{f}}{\partial \psi} \right|_{\psi_0, K_0} = \begin{pmatrix} -\frac{1}{2} & -\frac{1}{2} \\ -\frac{1}{2} & -\frac{1}{2} \end{pmatrix},$$

where \mathbf{f} is the vector field given by (38) with corresponding state vector $\boldsymbol{\psi} = (\psi_1, \psi_2)$. This linearization is non-degenerate since it has a simple zero eigenvalue. We set $v = \begin{pmatrix} 1 \\ -1 \end{pmatrix}$ and $w = \begin{pmatrix} 1 & -1 \end{pmatrix}$ to be respectively the right and left eigenvectors of the linearization for the zero eigenvalue.

2. *Transversality condition to control non-degeneracy with respect to the parameter.*

For this condition we check if the eigenvalues cross the imaginary axis with non-zero speed.

We compute

$$\frac{\partial^2 \mathbf{f}}{\partial \boldsymbol{\psi} \partial K} \Big|_{\boldsymbol{\psi}_0, K_0} = \frac{1}{2} \begin{pmatrix} 1 & -1 \\ -1 & 1 \end{pmatrix},$$

which implies that $w \cdot \frac{\partial^2 \mathbf{f}}{\partial \boldsymbol{\psi} \partial K} \Big|_{\boldsymbol{\psi}_0, K_0} \cdot v = 2 \neq 0$. Hence, the eigenvalues cross the imaginary axis with non-zero speed.

3. *Transversality condition to control non-degeneracy with respect to the dominant effect of the cubic nonlinear term.*

For this condition we compute

$$w_i v_j v_k v_l \frac{\partial^3 f_i}{\partial \psi_j \partial \psi_k \partial \psi_l} \Big|_{\boldsymbol{\psi}_0, K_0} = -6 < 0,$$

for all $i, j, k, l \in \{1, 2\}$ and f_i is the i th component of \mathbf{f} . Since we get a strictly negative number, the pitchfork is supercritical.

This last condition completes the proof of the existence of a codimension-one supercritical pitchfork bifurcation at $\boldsymbol{\psi} = (0, \pi)$, $K = 1$.

Before the bifurcation ($K < 1$), the only stable equilibrium is $\boldsymbol{\psi}_{antisync2} = (0, \pi)$. This corresponds to the case where each informed subgroup follows its own preferred direction; there is no compromise between the individuals and the group splits. When $K < 1$ the strength of the coupling force compared to the preferred direction is too weak to influence the stable steady state of the system. The motion of the group is the same as if there were no coupling between the two informed subgroups. For $K > 1$, there are two stable equilibria, $\boldsymbol{\psi}_{sync1}$ and $\boldsymbol{\psi}_{sync2}$. These

correspond, respectively, to the motion in the directions $\Psi = \frac{\bar{\theta}_2}{2} = \frac{\pi}{2}$ and $\Psi = \frac{\bar{\theta}_2}{2} + \pi = \frac{3\pi}{2}$. As we increase the bifurcation parameter K , the two directions ψ_1 and ψ_2 become synchronized. $\bar{\theta}_2 = \pi$ is the only case where we have two stable equilibria for large value of K .

7 Conclusion

We have modelled and studied equilibria, stability and bifurcations for a group of $N = N_1 + N_2 + N_3$ coupled individuals moving in the plane where there are N_1 informed individuals with a preferred direction $\bar{\theta}_1 = 0$, $N_2 = N_1$ informed individuals with a second preferred direction $\bar{\theta}_2$ and $N_3 = 0$ uninformed individuals. We showed that the system has either one or two stable equilibria. The K -almost synchronized motion of the two subgroups in the direction $\Psi = \frac{\bar{\theta}_2}{2}$ is always stable. For $K \in (K_1, K_0)$ and $\bar{\theta}_2 \in [\frac{\pi}{2}, \pi)$, the K -almost synchronized motion of the two subgroups in the direction $\Psi = \frac{\bar{\theta}_2}{2} + \pi$ is stable. We showed the existence of a hypercritical pitchfork bifurcation at $\psi_0 = (\frac{3\pi}{2}, \bar{\theta}_2 + \frac{\pi}{2})$, $K = 2/\sin \bar{\theta}_2$ when $\bar{\theta}_2 \in [\frac{\pi}{2}, \pi)$. In the case $\bar{\theta}_2 = \pi$ we proved a supercritical pitchfork at $\psi = (0, \pi)$, $K = 1$. At $\psi = (\frac{3}{2}, \pi)$, $K = 2$ and $\bar{\theta}_2 = \frac{\pi}{2}$, the system was proved to have a highly degenerate bifurcation point with its linearization equal to the zero matrix. This bifurcation was investigated in the $(\bar{\theta}_2, \psi_i)$ plane and was shown to be an elliptic umbilic catastrophe.

In the case $N_1 \neq N_2$, the persistent stable equilibrium does not correspond to $\Psi = \frac{\bar{\theta}_2}{2}$, but rather it is a weighted average of 0 and $\bar{\theta}_2$. For example, if $N_1 > N_2$, the stable solution Ψ corresponds to a direction closer to 0 than to $\bar{\theta}_2$. For N_2 fixed, the stable equilibrium value of Ψ asymptotically approaches 0 for increasing N_1 as shown in Figure 11. Likewise for N_1 fixed, the stable equilibrium value of Ψ asymptotically approaches $\bar{\theta}_2$ for increasing N_2 .

In [19] extensions of this homogeneous model are investigated by introducing heterogeneity. Heterogeneity is considered both in the context of informed and uninformed individuals. With either type of heterogeneity, both the time-scale separation and the lumped behavior remain unchanged. Indeed some of the very same bifurcations proven in the present paper are recovered numerically in [19] suggesting a measure of robustness to the results here.

The continuous model in this paper presents several simplifications as compared to the discrete time model in [3]. First we constrain our study to the phase dynamics of the individuals rather than the full spatial dynamics. Also we assume that the individuals can be influenced by all other

individuals (not just ones nearby). Finally we perform the bifurcation analysis of the system in the absence of uninformed individuals. Our continuous model, like the discrete time model in [3], shows that consensus is possible within a group of individuals with conflicting information and without signalling or identification of informed individuals. However, unlike the discrete-time model with uninformed individuals, the continuous model restricted to informed individuals only (i.e., $N_3 = 0$) does not exhibit full synchronization of the group unless the coupling gain K is very large (equivalent to the weight ω of the preferred direction in [3] being very small). This means that for large weight on the preferred direction in the model (1) with $N_3 = 0$, the individuals in the population do not fully aggregate and the group splits. Also it never happens, in the case of equal populations for the two informed subgroups ($N_1 = N_2$), that the group selects to move as a whole in one of the preferred directions.

On the other hand, if we introduce feedback on the gain K , analogous to the feedback on the weight ω in [3], which reinforces (diminishes) the gain if individuals find themselves moving in (away from) their preferred direction, then simulation results resemble more closely those in [3]. I.e., in this case there is consensus without a large K and the group chooses one or the other of the preferred directions.

Simulations also suggest that even without the feedback on the gain K , the model will exhibit results closer to those in [3] when we reintroduce the dynamics of the uninformed individuals. Of particular interest are uninformed individuals that are influenced only by near neighbors or perhaps only by those that are moving in front of them. In this case, we might expect that as a function of initial conditions, the uninformed individuals could be “won over” by one of the two informed subgroups. Then, in effect, the “winning” informed subgroup will appear in the model to have its membership greatly increased. In this case, just like the case $N_1 > N_2$ discussed above, the group will move in a weighted average direction that is close to the preferred direction as long as the number of uninformed individuals is large as compared to uninformed individuals in the “losing” subgroup.

The dependency on the angle between the two preferred directions revealed in the discrete-time model might also be reasonably recovered with the reintroduction of uninformed individuals. Recall that in [3] at small differences between the two preferred directions, the group moves in the average direction while at large differences, the group moves in one or the other preferred direction. It

seems quite reasonable, for small differences in preferred direction in the continuous model with uninformed individuals, that the uninformed individuals may not be won over by either informed subgroup and instead contribute to consensus at the average. Whereas at large differences between preferred directions, the discussion above might apply so that the group effectively picks one of the preferred directions.

In ongoing work, motivated by these simulation studies that identify critical factors contributing to aggregation and group decision making, we are developing and studying the dynamics of models that include both uninformed individuals and limited interconnections between individuals within the group. We are investigating, for example, in the case that the group chooses one of the preferred directions, how the naive population gets won over by one informed subgroup.

As the continuous model grows to better resemble the behavior of the natural system, the value of the analysis will increase. Prediction of stability and bifurcation of solutions, analogous to those in the present paper, have the potential to provide new insights by going beyond regions of phase space explored with discrete simulation.

References

- [1] J. Krause and G. D. Ruxton. *Living in Groups*. Oxford Univ. Press, Oxford, 2002.
- [2] I. D. Couzin and J. Krause. Self-organization and collective behaviour in vertebrates. *Advances in the Study of Behavior*, 32:1–75, 2003.
- [3] I.D. Couzin, J. Krause, N.R. Franks, and S.A. Levin. Effective leadership and decision making in animal groups on the move. *Nature*, 434:513–516, 2005.
- [4] E. Justh and P. S. Krishnaprasad. Equilibria and steering laws for planar formations. *Systems and Control Letters*, 52:1:25–38, 2004.
- [5] R. Sepulchre, D. Paley, and N. E. Leonard. Stabilization of planar collective motion: All-to-all communication. *IEEE Trans. Automatic Control*, 52(5):811–824, 2007.
- [6] N. E. Leonard, D. Paley, F. Lekien, R. Sepulchre, D. Fratantoni, and R. Davis. Collective motion, sensor networks and ocean sampling. *Proceedings of the IEEE*, 95(1):48–74, 2007.

- [7] E. Biyik and M. Arcak. Area aggregation and time scale modeling for sparse nonlinear networks. *Proceedings of the 45th IEEE Conference on Decision and Control*, pages 4046–4051, 2006.
- [8] R. Sepulchre, D. Paley, and N.E. Leonard. Stabilization of planar collective motion with limited communication. *IEEE Trans. Automatic Control*, 2007. To appear. Available online at <http://www.princeton.edu/~naomi>.
- [9] Y. Kuramoto. *Chemical oscillations, waves, and turbulence*. Springer-Verlag, 1984.
- [10] R. E. Mirollo and S. H. Strogatz. Jump bifurcation and hysteresis in an infinite-dimensional dynamical system of coupled spins. *SIAM J. Appl. Math.*, 50(1):108–124, 1990.
- [11] J.L. Cardy and S. Ostlund. Random symmetry-breaking fields and the XY model. *Phys. Rev. B*, 25:6899–6909, 1982.
- [12] S. H. Strogatz. From Kuramoto to Crawford: Exploring the onset of synchronization in populations of coupled oscillators. *Physica D*, 143:1–20, 2000.
- [13] H. K. Khalil. *Nonlinear Systems 3rd ed.* Prentice Hall, 2002.
- [14] J. Guckenheimer and P. Holmes. *Nonlinear Oscillations, Dynamical Systems, and Bifurcations of Vector Fields*. Springer-Verlag, New York, 1983.
- [15] R. Thom. *Structural Stability and Morphogenesis*. Benjamin, New York, 1972.
- [16] T. Poston and I. Stewart. *Catastrophe Theory and its Applications*. Pitman, London, 1978.
- [17] M. Lindauer. Communication in swarm-bees searching for a new home. *Nature*, 179:63–67, 1957.
- [18] S. Strogatz. *Nonlinear Dynamics and Chaos*. Perseus, 1994.
- [19] S. J. Moon, B. Nabet, N. E. Leonard, S. A. Levin, and I. G. Kevrekidis. Heterogeneous animal group models and their group-level alignment dynamics; an equation-free approach. *J. Theoretical Biology*, 246:100–112, 2007.

A Proof of well-defined change of variables

In this appendix, we show that the change of variables $\boldsymbol{\theta} \mapsto (\boldsymbol{\alpha}^1, \psi_1, \boldsymbol{\alpha}^2, \psi_2, \boldsymbol{\alpha}^3, \psi_3)$ from Section 2.2 is well defined near the manifold \mathcal{M} , where \mathcal{M} is the invariant manifold of (1) defined by $\theta_j = \psi_k$, $j \in \mathcal{N}_k$, $k = 1, 2, 3$. We write $(\boldsymbol{\alpha}^1, \psi_1, \boldsymbol{\alpha}^2, \psi_2, \boldsymbol{\alpha}^3, \psi_3) = F(\boldsymbol{\theta})$ and prove that F is locally invertible near \mathcal{M} . On \mathcal{M} , we have

$$\begin{aligned}
 \left. \frac{\partial \alpha_{j(k,l)}}{\partial \theta_m} \right|_{\mathcal{M}} &= -i && \text{if } m \neq j(k,l) \\
 &= (N_k - 1)i && \text{if } m = j(k,l) \\
 &= 0 && \text{otherwise} \\
 \left. \frac{\partial \psi_k}{\partial \theta_m} \right|_{\mathcal{M}} &= \frac{1}{N_k} && \text{if } m \in \mathcal{N}_k \\
 &= 0 && \text{otherwise.}
 \end{aligned} \tag{A-1}$$

Using (A-1), the Jacobian of F evaluated on \mathcal{M} can be written as

$$\left. \frac{dF}{d\boldsymbol{\theta}} \right|_{\mathcal{M}} = \begin{pmatrix} A_1 & \mathbf{0}_{N_1, N_2} & \mathbf{0}_{N_1, N_3} \\ \mathbf{0}_{N_2, N_1} & A_2 & \mathbf{0}_{N_2, N_3} \\ \mathbf{0}_{N_3, N_1} & \mathbf{0}_{N_3, N_2} & A_3 \end{pmatrix},$$

where

$$A_k = \begin{pmatrix} (N_k - 1)i & -i & \cdots & \cdots & -i \\ -i & \ddots & \ddots & -i & \vdots \\ \vdots & \ddots & \ddots & \ddots & \vdots \\ -i & \cdots & -i & (N_k - 1)i & -i \\ \frac{1}{N_k} & \cdots & \cdots & \cdots & \frac{1}{N_k} \end{pmatrix} \in \mathbb{R}^{N_k \times N_k}.$$

Each A_k and hence $\frac{dF}{d\theta}|_{\mathcal{M}}$ is invertible with

$$A_k^{-1} = \begin{pmatrix} -\frac{i}{N_k} & 0 & \cdots & 0 & \frac{2}{N_k} \\ 0 & \ddots & \ddots & \vdots & \vdots \\ \vdots & \ddots & \ddots & 0 & \vdots \\ 0 & \cdots & 0 & -\frac{i}{N_k} & \vdots \\ \frac{i}{N_k} & \cdots & \cdots & \frac{i}{N_k} & \frac{2}{N_k} \end{pmatrix} \in \mathbb{R}^{N_k \times N_k}. \quad (\text{A-2})$$

This concludes the proof that $F : \theta \mapsto (\alpha^1, \psi_1, \alpha^2, \psi_2, \alpha^3, \psi_3)$ is locally invertible in a neighborhood of \mathcal{M} . Hence the change of variables from $\theta \mapsto (\alpha^1, \psi_1, \alpha^2, \psi_2, \alpha^3, \psi_3)$ is well defined near \mathcal{M} .

B Proof of the attractivity of the slow manifold

In this appendix, we show that \mathcal{M} , the invariant manifold of (1) defined by $\theta_j = \psi_k$, $j \in \mathcal{N}_k$, $k = 1, 2, 3$, is attractive. This is done by proving for the boundary layer dynamics

$$\frac{d\alpha_j}{dt} = g_j(\alpha^1, \alpha^2, \alpha^3, \psi_1, \psi_2, \psi_3, 0), \quad j \in \mathcal{N}_k, j \neq j_{(k, N_k)}, k = 1, 2, 3,$$

local exponential stability uniformly in ψ_1, ψ_2, ψ_3 of the invariant manifold \mathcal{M} .

The boundary layer dynamics can be written as

$$\begin{aligned} \dot{\alpha}_j &= iN_1\alpha_j \left(-\frac{N_1}{N}\rho_1 \sin(\psi_1 - \theta_j) + \frac{N_2}{N}\rho_2 \left(\sin(\psi_2 - \theta_j) - \rho_1 \sin(\psi_2 - \psi_1) \right) \right. \\ &\quad \left. + \frac{N_3}{N}\rho_3 \left(\sin(\psi_3 - \theta_j) - \rho_1 \sin(\psi_3 - \psi_1) \right) \right), \quad j \in \mathcal{N}_1, j \neq j_{(1, N_1)} \\ \dot{\alpha}_j &= iN_2\alpha_j \left(-\frac{N_2}{N}\rho_2 \sin(\psi_2 - \theta_j) + \frac{N_1}{N}\rho_1 \left(\sin(\psi_1 - \theta_j) - \rho_2 \sin(\psi_1 - \psi_2) \right) \right. \\ &\quad \left. + \frac{N_3}{N}\rho_3 \left(\sin(\psi_3 - \theta_j) - \rho_2 \sin(\psi_3 - \psi_2) \right) \right), \quad j \in \mathcal{N}_2, j \neq j_{(2, N_2)} \\ \dot{\alpha}_j &= iN_3\alpha_j \left(-\frac{N_3}{N}\rho_3 \sin(\psi_3 - \theta_j) + \frac{N_1}{N}\rho_1 \left(\sin(\psi_1 - \theta_j) - \rho_3 \sin(\psi_1 - \psi_3) \right) \right. \\ &\quad \left. + \frac{N_2}{N}\rho_2 \left(\sin(\psi_2 - \theta_j) - \rho_3 \sin(\psi_2 - \psi_3) \right) \right), \quad j \in \mathcal{N}_3, j \neq j_{(3, N_3)}. \end{aligned}$$

The linearization of the boundary layer model is given by

$$\frac{\partial \dot{\alpha}_j}{\partial \alpha_m} \Big|_{\mathcal{M}} = -i \frac{N_k}{N} \left(\frac{\partial \theta_j}{\partial \alpha_m} \Big|_{\mathcal{M}} \left(N_k + \sum_{l \neq k} N_l \cos(\psi_l - \psi_k) \right) + \frac{\partial \rho_k}{\partial \alpha_m} \Big|_{\mathcal{M}} \sum_{l \neq k} N_l \sin(\psi_l - \psi_k) \right),$$

$$j \in \mathcal{N}_k, j \neq j_{(k, N_k)}, k = 1, 2, 3, m \in \{1, \dots, N\} \setminus \{j_{(1, N_1)}, j_{(2, N_2)}, j_{(3, N_3)}\}.$$
(B-1)

Using equation (A-2), the values for $\frac{\partial \theta_j}{\partial \alpha_m} \Big|_{\mathcal{M}}$ can be read as

$$\frac{\partial \theta_j}{\partial \alpha_m} \Big|_{\mathcal{M}} = -\frac{i}{N_k} \quad \text{if } m = j$$

$$= 0 \quad \text{otherwise.}$$
(B-2)

Taking partial derivatives with respect to α_m of equation (2) yields

$$\frac{\partial \rho_k}{\partial \alpha_m} e^{i\psi_k} + \rho_k i \frac{\partial \psi_k}{\partial \alpha_m} e^{i\psi_k} = \frac{i}{N_k} \sum_{j \in \mathcal{N}_k} \frac{\partial \theta_j}{\partial \alpha_m} e^{i\theta_j}.$$
(B-3)

Evaluating (B-3) on \mathcal{M} and using equation (A-2) gives

$$\frac{\partial \rho_k}{\partial \alpha_m} \Big|_{\mathcal{M}} = \frac{i}{N_k} \sum_j \frac{\partial \theta_j}{\partial \alpha_m} \Big|_{\mathcal{M}} = 0.$$
(B-4)

Plugging equation (B-2) and (B-4) into (B-1), the Jacobian can be rewritten as a diagonal matrix J with

$$J_{jj} = -\frac{1}{N} \left(N_k + \sum_{l \neq k} N_l \cos(\psi_l - \psi_k) \right), \quad j \in \mathcal{N}_k, j \neq j_{(k, N_k)}, k = 1, 2, 3.$$

When $N_1 = N_2$ and $N_3 = 0$, this matrix has all its eigenvalues strictly negative. This concludes the proof that the boundary layer dynamics are locally exponentially stable uniformly in ψ_1, ψ_2, ψ_3 at the invariant manifold \mathcal{M} . Hence, \mathcal{M} the invariant manifold of (1) defined by $\theta_j = \psi_k, j \in \mathcal{N}_k, k = 1, 2, 3$, is attractive.

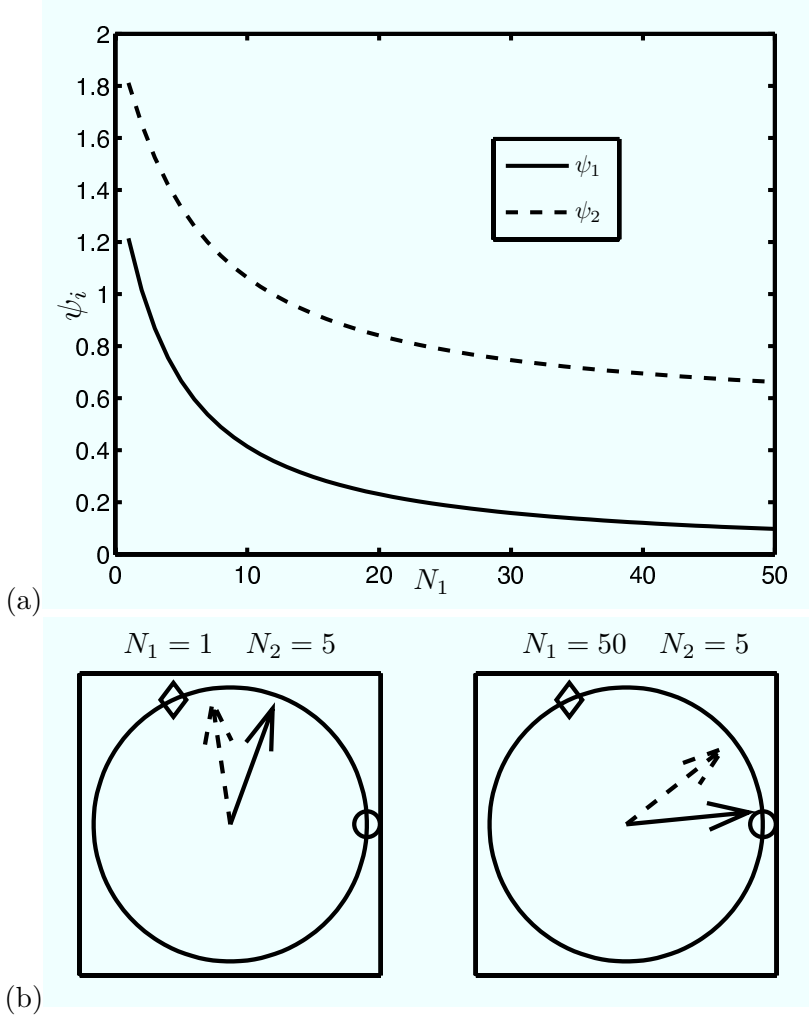


Figure 11: (a) The equilibrium values of ψ_1 and ψ_2 corresponding to the stable motion ψ_{sync1} as a function of subgroup population size N_1 for fixed subgroup population size $N_2 = 5$. As N_1 increases the stable equilibrium values of both ψ_1 and ψ_2 approach 0, the preferred direction $\bar{\theta}_1$ of the subgroup with dominating population size N_1 . (b) The stable equilibrium ψ_{sync1} for the two extreme values of N_1 . The motion of the group is closer to $\bar{\theta}_2 = 2$ rad when $1 = N_1 < N_2 = 5$. The motion of the group is closer to $\bar{\theta}_1 = 0$ rad when $50 = N_1 > N_2 = 5$.